

DOE/BC/14884-12
Distribution Category UC-122

Surfactant Loss Control in Chemical Flooding
Spectroscopic and Calorimetric Study of
Adsorption and Precipitation on Reservoir Minerals

Annual Report for the Period
September 30, 1993 to September 30, 1994

By
P. Somasundaran

June 1995

Work Performed Under Contract No. DE-AC22-92BC14884

Prepared for
U.S. Department of Energy
Assistant Secretary for Fossil Energy

Jerry Casteel, Project Manager
Bartlesville Project Office
P.O. Box 1398
Bartlesville, OK 74005

Prepared by
Columbia University
Box 20, Low Memorial Library
New York, NY 10027

DISTRIBUTION OF THIS DOCUMENT IS UNLIMITED

MASTER⁰²

THE UNIVERSITY OF CHICAGO PRESS

CHICAGO, ILLINOIS

DISCLAIMER

This report was prepared as an account of work sponsored by an agency of the United States Government. Neither the United States Government nor any agency thereof, nor any of their employees, make any warranty, express or implied, or assumes any legal liability or responsibility for the accuracy, completeness, or usefulness of any information, apparatus, product, or process disclosed, or represents that its use would not infringe privately owned rights. Reference herein to any specific commercial product, process, or service by trade name, trademark, manufacturer, or otherwise does not necessarily constitute or imply its endorsement, recommendation, or favoring by the United States Government or any agency thereof. The views and opinions of authors expressed herein do not necessarily state or reflect those of the United States Government or any agency thereof.

DISCLAIMER

Portions of this document may be illegible in electronic image products. Images are produced from the best available original document.

TABLE OF CONTENTS

LIST OF FIGURES	4
LIST OF TABLES	7
LIST OF SYMBOLS	8
ABSTRACT	9
EXECUTIVE SUMMARY	10
MATERIALS & METHODS	12
Materials	12
Minerals	12
Other Chemicals	12
Methods	12
Analytical Techniques	12
Adsorption	13
Surface tension	13
Zeta potential	13
Fluorescence spectroscopy	13
RESULTS & DISCUSSION	15
Adsorption/Desorption of Cationic Surfactant at the alumina-water interface	15
Desorption of cationic surfactant from alumina-water interface	20
Adsorption of cationic-nonionic surfactant mixtures	23
Theoretical and Thermodynamic Modelling	33
Solution behavior of surfactant mixtures	33
Desorption of surfactant mixtures from alumina-water interface	40
Sodium dodecyl sulfate (SDS)/ C ₁₂ EO ₈ mixture adsorption	46
Fluorescence Probing of Mixed-surfactant Adsorbed Layers	50
SUMMARY	56

LIST OF FIGURES

Figure 1	Adsorption isotherm of tetradecyl trimethylammonium chloride (TTAC) on alumina at pH 10.	15
Figure 2	Zeta potential of alumina after adsorption of tetradecyl trimethyl ammonium chloride (TTAC) at pH 10.	16
Figure 3	Settling rate of alumina suspensions after tetradecyl trimethyl ammonium chloride (TTAC) adsorption at pH 10.	17
Figure 4	Adsorption isotherm of tetradecyl trimethylammonium chloride (TTAC) on alumina and corresponding changes in pyrene monomer fluorescence from the alumina water interface and the supernatant.	19
Figure 5	Desorption of TTAC from alumina upon dilution from different residual concentrations (C_r).	20
Figure 6	Changes in pyrene polarity parameter from the TTAC adsorbed layer on alumina upon dilution from different residual concentrations and also in bulk solution.	22
Figure 7	Adsorption isotherms of pentadecylethoxylated nonyl phenol (NP-15) on alumina: with preadsorbed amounts of tetradecyl trimethylammonium chloride (TTAC), and when added together with TTAC.	24
Figure 8	Adsorption of tetradecyl trimethyl ammonium chloride (TTAC) in the presence and absence of NP-15.	26
Figure 9	Adsorption of pentadecylethoxylated nonylphenol (NP-15) on alumina in presence of varying amounts of tetradecyltrimethylammonium chloride (TTAC).	27
Figure 10	Total adsorption of surfactant mixtures at the alumina-water interface.	29
Figure 11	Zeta-potential of alumina after adsorption of TTA:NP-15 mixtures of different composition.	30
Figure 12	Ratio of adsorption densities of TTAC:NP-15 for different mixtures.	31
Figure 13	Surface tension of TTAC:NP-15 surfactant mixtures after adsorption.	32
Figure 14	Surface tension of solutions of TTAC, NP-15 and their mixtures.	32
Figure 15	Regular solution and ideal mixing theory for determining the interaction parameter for the tetradecyl trimethylammoniumchloride (TTAC) pentadecylethoxylated nonyl	

	phenol (NP-15) system.	37
Figure 16	Monomer concentrations of tetradecyl trimethylammoniumchloride (TTAC) in mixtures with pentadecylethoxylated nonyl phenol (NP-15) calculated using regular solution theory with an interaction parameter -1.5	38
Figure 17	Monomer concentrations of pentadecylethoxylated nonyl phenol (NP-15) in mixtures with tetradecyl trimethylammonium chloride (TTAC) calculated using regular solution theory with an interaction parameter = -1.5.	39
Figure 18	Desorption of tetradecyl trimethyl ammonium chloride (TTAC) from mixed adsorbed layer on alumina upon dilution from different residual concentrations of TTAC (C_r). TTAC:NP-15 = 4:1	40
Figure 19	Desorption of pentadecyl ethoxylated nonyl phenol (NP-15) from alumina upon dilution from different residual concentrations (C_r). TTAC:NP-15 ratio = 4:1. .	41
Figure 20	Desorption of tetradecyl trimethylammonium chloride (TTAC) from alumina-water interface upon dilution from different residual concentrations (C_r) in presence of 1:1 pentadecyl ethoxylated nonyl phenol (NP-15).	42
Figure 21	Desorption of pentadecylethoxylated nonyl phenol (NP-15) upon dilution from different residual concentrations (C_r) in presence of 1:1 tetradecyl trimethylammonium chloride (TTAC).	43
Figure 22	Desorption of tetradecyl trimethyl ammonium chloride (TTAC) from alumina upon dilution from different residual concentrations (C_r). TTAC:NP-15 ratio = 1:4. .	44
Figure 23	Desorption of pentadecyl ethoxylated nonyl phenol (NP-15) from alumina upon dilution from different residual concentrations (C_r). TTAC:NP-15 ratio = 1:4. .	45
Figure 24	Effect of nonionic surfactant hydrocarbon chain length on the adsorption of sodium dodecyl sulfate (SDS) on kaolinite from 1:1 SDS/ C_n EO ₈ mixtures	47
Figure 25	Effect of hydrocarbon chain length (C_n EO ₈) on the adsorption of nonionic surfactant on kaolinite. 0.03 M NaCl, pH 5.	48
Figure 26	Effect of nonionic surfactant hydrocarbon chain length on the adsorption of C_n EO ₈ (n=10,12,14,16) on kaolinite from its 1:1 mixtures with SDS. 0.03 M NaCl, pH 5	49

Figure 27	Schematic representation of the effect of nonionic surfactant hydrocarbon chain length on the adsorption of the anionic surfactant SDS when the nonionic surfactant hydrocarbon chain is (a) longer than, (b) equal to and (c) shorter than SDS. . . .	49
Figure 28	Total adsorption of sodium dodecyl sulfate (SDS) and 1:1 SDS/C ₁₂ EO ₈ mixtures on alumina and aggregation numbers of surfactant.	52
Figure 29	Isotherms for individual surfactant adsorption on alumina from 1:1 SDS/C ₁₂ EO ₈ mixtures.	54

LIST OF TABLES

Table I	Calculated results of x and C^* by regular solution theory	35
Table II	Aggregation number (N_{agg}) of Surfactant micelles, 0.03 M NaCl, 25°C	53
Table III	Surfactant aggregation number (N_{agg}) for the adsorption of 1:1 SDS/ $C_{12}EO_8$ mixture on alumina: 0.03 M NaCl, pH 6.5, 25°C	55

LIST OF SYMBOLS

- α : mole fraction of surfactant 1 in the mixed surfactant solution
- β : interaction parameter defined in the regular solution theory
- f_i : activity coefficient of surfactant i in mixed micelles
- N_A : Avogadro number
- w_{ij} : the energies of interaction between surfactant species i & j in the mixed micelles
- x : mole fraction of surfactant 1 in mixed micelles
- C_i : CMCs of pure surfactant i
- C : total concentration of mixed surfactant
- C^* : CMC of mixed surfactant
- C_i^m : the monomer concentration of surfactant i
- I_3/I_1 : polarity parameter
- P : pyrene molecule in its ground state
- P^* : pyrene molecule in its excited state
- I_t : pyrene fluorescence emission intensity at desired wavelength at time t
- I_0 : pyrene fluorescence emission intensity at desired wavelength at time $t=0$
- k_0 : the monomer decay rate constant
- k_e : the excimer formation rate constant
- N_{agg} : the aggregation number of the surfactant aggregate (micelle or hemimicelle)
- C_i : the total initial surfactant concentration
- C_r : the total residual surfactant concentration
- $[Py]$: the pyrene concentration
- n : average number of pyrene molecule per surfactant aggregate

ABSTRACT

The aim of this project is to elucidate the mechanisms underlying adsorption and surface precipitation of flooding surfactants on reservoir minerals. Effect of surfactant structure, surfactant combinations, other inorganic and polymeric species is being studied. A multi-pronged approach consisting of micro & nano spectroscopy, microcalorimetry, electrokinetics, surface tension and wettability is used to achieve the goals. The results of this study should help in controlling surfactant loss in chemical flooding and also in developing optimum structures and conditions for efficient chemical flooding processes.

During the second year of this three year contract, adsorption/desorption of single surfactants and select surfactant mixtures on alumina and silica was studied. Surfactants studied include the anionic sodium dodecyl sulfate (SDS), cationic tetradecyl trimethyl ammonium chloride (TTAC), nonionic pentadecylethoxylated nonyl phenol (NP-15) and the nonionic octaethylene glycol n-dodecyl ether ($C_{12}EO_8$) of varying hydrocarbon chain length. The microstructure of the adsorbed layer in terms of micropolarity and aggregation numbers was probed using fluorescence spectroscopy. Changes of microstructure upon dilution (desorption) were also studied. Presence of the nonionic surfactant in the mixed aggregate led to shielding of the charge of the ionic surfactant which in-turn promoted aggregation but reduced electrostatic attraction between the charged surfactant and the mineral surface. Strong consequences of surfactant interactions in solution upon adsorption as well as correlations between monomer concentrations in mixtures and adsorption were revealed.

EXECUTIVE SUMMARY

During this year, adsorption/desorption of single surfactants (anionic and cationic) as well as their mixtures with non-ionic surfactants on minerals was studied, and some beneficial results of the interactions between the surfactants have become noted. Adsorption/desorption of surfactants and their mixtures was correlated with changes in the interfacial behavior such as wettability and zeta potential and mechanisms involved were explored.

Effect of the most important variable, hydrocarbon chain length, of a nonionic surfactant, octaethylene glycol mono-n-alkyl ether (C_nEO_8) on the adsorption of the anionic sodium dodecylsulfate (SDS) was studied. The nonionic surfactant enhanced the adsorption of the anionic surfactant, but interestingly only when the hydrocarbon chain length was less than or equal to that of the latter. Results are discussed in terms of the hydrocarbon chain-chain interaction and shielding of the chains from hydrophilic environments. This shielding leads to an increase in the size of the adsorbed aggregate of 1:1 mixtures of SDS/ $C_{12}EO_8$ at the alumina-water interface as measured by fluorescence spectroscopy. Computation of individual aggregate size from the ratio of adsorption densities at the interface (and the total aggregate size) leads to the resolution that the sodium dodecylsulfate (SDS) aggregate is smaller than the octaethylene glycol mono-n-dodecyl ether ($C_{12}EO_8$) aggregate.

Adsorption/desorption of mixtures of tetradecyltrimethylammonium chloride (TTAC) and pentadecylethoxylatednonylphenol (NP-15) at the alumina water interface was studied. While NP-15 does not adsorb on alumina by itself, it was forced to adsorb by preadsorbed and coadsorbing TTAC. Interestingly coadsorbing TTAC had a higher influence on the adsorption of NP-15 than preadsorbed TTAC suggesting the importance of the dynamics of the adsorption process. With an increase in

pentadecylethoxylatednonylphenol (NP-15) content in the mixtures, adsorption of TTAC was reduced due to steric repulsion and competition for adsorption sites. In order to understand the dynamics and reversibility, desorption of TTAC from the alumina surface was studied in the presence and absence of NP-15. For the case of TTAC alone, it was found that adsorbed aggregates reorganized at the alumina-water interface. In the presence of NP-15 it was observed that in TTAC rich mixtures, the desorption of TTAC is similar to that of TTAC alone. As the adsorption of NP-15 was dependent on the presence of TTAC, the desorption also was TTAC dependent except in the case of NP-15 rich mixtures. Regular solution theory was used to model interactions between NP-15 and TTAC in solutions and model was extend to the adsorption behavior of the mixture.

Interactions between surfactants can be exploited to monitor the adsorption/desorption behavior and the aggregation tendencies of the individual surfactants. In the case of anionic-nonionic as well as cationic-nonionic surfactant mixtures, hydrophobic interaction between the chains was the dominant mechanism which led to the synergistic interactions. The presence of the nonionic surfactant in a surfactant mixture shields the charge of the ionic surfactant thus promoting aggregation as well as reducing electrostatic attraction between the charged surfactant and the substrate.

MATERIALS & METHODS

Materials

Surfactants: Anionic, cationic and nonionic surfactants were studied. Sodium dodecyl sulfate (SDS) of greater than 99% purity purchased from Fluka chemicals was used as received. The nonionic surfactants covered a wide range of hydrophobic and hydrophilic chain lengths and were purchased from Nikko Chemicals. The ethoxylated alcohols were of the general structure $C_nH_{2n+1}(CH_2CH_2O)_mH$ or C_nEO_m . The homologues studied were $C_{10}EO_8$, $C_{12}EO_8$, $C_{14}EO_8$, and $C_{16}EO_8$ thus providing an opportunity for studying the effect of surfactant structure on mixture adsorption. The cationic surfactant n-tetradecyl trimethyl ammonium chloride, $[CH_3(CH_2)_{13}N(CH_3)_3]Cl$ (TTAC), from American Tokyo Kasei, Inc., and the nonionic pentadecylethoxylated nonyl phenol, $C_9H_{19}C_6H_4O(CH_2CH_2O)_{15}H$ (NP-15), from Nikko Chemicals, Japan were used as received.

Minerals

Mineral	Surface area (m ² /g)	Supplier	Particle size (μm)
Kaolinite	8.2	Univ. of Missouri	--
Alumina	15.0	Linde (Union Carbide)	0.3
Silica	25.0	Spherosil	40 - 100

Other Chemicals: Pyrene was obtained from Aldrich Chemicals and recrystallized from ethanol. NaCl, HCl and NaOH used were of ACS reagent grade. All solutions were prepared in triply distilled water and at constant ionic strength as indicated in later sections.

Methods

Analytical Techniques: Sodium dodecyl sulfate (SDS) concentration was determined using a two-

phase titration method¹. Tetradecyl trimethyl ammonium chloride (TTAC) concentration was determined by complexing the surfactant with excess SDS and measuring the non-complexed SDS using the two-phase titration. The concentration of ethoxylated alcohol (C_nEO_m) was determined using high pressure liquid chromatography (HPLC) with a C_{18} bonded silica column and a refractive index detector. The solvent used was a 90:10 mixture of acetonitrile and water. Pentadecylethoxylated nonyl phenol concentration was determined by UV absorption at 223 nm.

Adsorption: Adsorption experiments were conducted in 25 ml Teflon capped scintillation vials. One gram of the solid was brought in contact with 5 ml of solution of desired ionic strength for 2 hours. Next, 5 ml of salt solution containing surfactant or surfactant mixture of desired concentration was added. The system was conditioned on a wrist action shaker 15 h in the case of silica, 24 h in the case of alumina and 72 h in the case of kaolinite. The suspensions were then centrifuged at 3000-4000 rpm and the supernatant analyzed for residual concentration. Adsorption was calculated based upon surfactant depleted from solution.

Desorption: The desorption tests consisted of conditioning of supernatants of slurries from adsorption tests for 15 hours with the desired amounts of diluents adjusted for pH and ionic strength. This procedure was repeated several times depending upon the concentration.

Surface tension: Surface tension of surfactant solutions was measured using a Wilhelmy plate or a du Nuoy ring tensiometer.

Zeta potential: Zeta potential of mineral particles before and after adsorption were made on a PEN KEM, Inc. Laser zee meter model 501 system.

Fluorescence spectroscopy: A Photon Technology International PTI LS-100 was used for

¹Z. Li and M.J. Rosen, *Analytical Chemistry*, **53**, 1981, 1516.

fluorescence experiments. The samples containing pyrene dissolved to its maximum solubility in water ($\approx 2 \times 10^{-7}$ kmol/m³) were excited at 335 nm and emission between 365 and 500 nm was recorded.

Solution conditions: All experiments were conducted at an ionic strength of 0.03 M NaCl and at a pH of 10.0 ± 0.5 . Triply distilled water of conductivity in the range of $(1-2) \times 10^{-6} \Omega^{-1}$ was used for preparing all solutions.

RESULTS & DISCUSSION

Adsorption/Desorption of Cationic Surfactant at the alumina-water interface

The adsorption/desorption behavior of a cationic surfactant (tetradecyltrimethylammonium chloride - TTAC) at the alumina water surface was studied in the presence and absence of a cosurfactant, nonionic pentadecylethoxylatednonylphenol (NP-15). Adsorption behavior was correlated with changes in interfacial properties such as zeta potential and stability. The microstructure of the adsorbed layers was probed using fluorescence spectroscopy.

The adsorption isotherm of TTAC on alumina at pH 10.5 is shown in figure 1. At this pH the alumina surface is negatively charged and the electrostatic attraction with the cationic TTAC will be dominant. There is a sharp increase in the adsorption density at around $5 \times 10^{-4} \text{ kmol/m}^3$ which is attributed to the formation of surfactant aggregates (hemimicelles) at the solid-liquid interface.

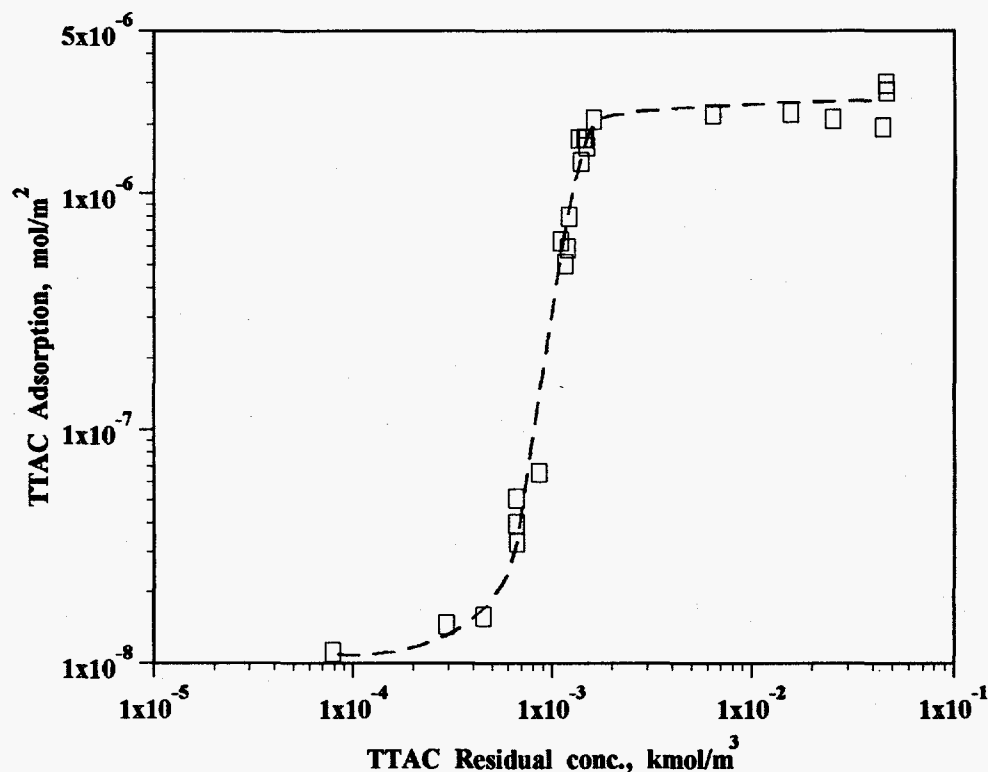


Figure 1 Adsorption isotherm of tetradecyl trimethylammonium chloride (TTAC) on alumina at pH 10.

The maximum adsorption density of tetradecyltrimethylammonium chloride (TTAC) on alumina at pH 10 is about $2.5 \times 10^{-6} \text{ mol/m}^2$. This translates to roughly $66 \text{ \AA}^2/\text{molecule}$ which is similar to the reported molecular area at the air/solution interface (61 \AA^2)². Comparing the zeta potential to the adsorption at the same residual concentrations, it can be seen that the charge of alumina is neutralized at a very low adsorption density of TTAC (figure 2). The fact that adsorption of the cationic tetradecyltrimethylammonium chloride (TTAC) continues to take place leading to monolayer coverage even after the particles have become similarly charged suggests the predominating role of hydrophobic interactions between the hydrocarbon tails in causing the adsorption.

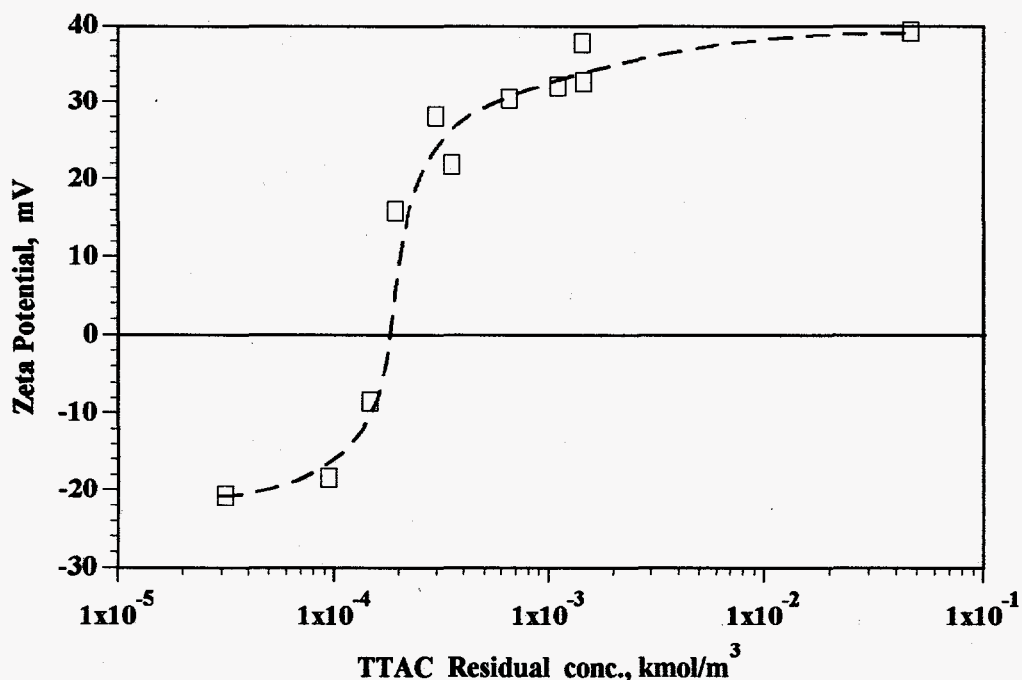


Figure 2 Zeta potential of alumina after adsorption of tetradecyl trimethyl ammonium chloride (TTAC) at pH 10.

The settling rate of the alumina suspensions after TTAC adsorption at pH 10 was measured and the results obtained are shown in figure 3. In the absence of and at low surfactant adsorption

²R.L. Venabl and R.V. Naumann, *J. Phys. Chem.*, **68**, 1964, 3498.

densities, the alumina suspension in water is dispersed and the settling rate is low. Once the surfactant forms aggregates at the interface, the alumina surface becomes hydrophobic and the settling rate is markedly increased which upon correlation with figures 1 and 2 can be attributed to hydrophobic bridging between particles³.

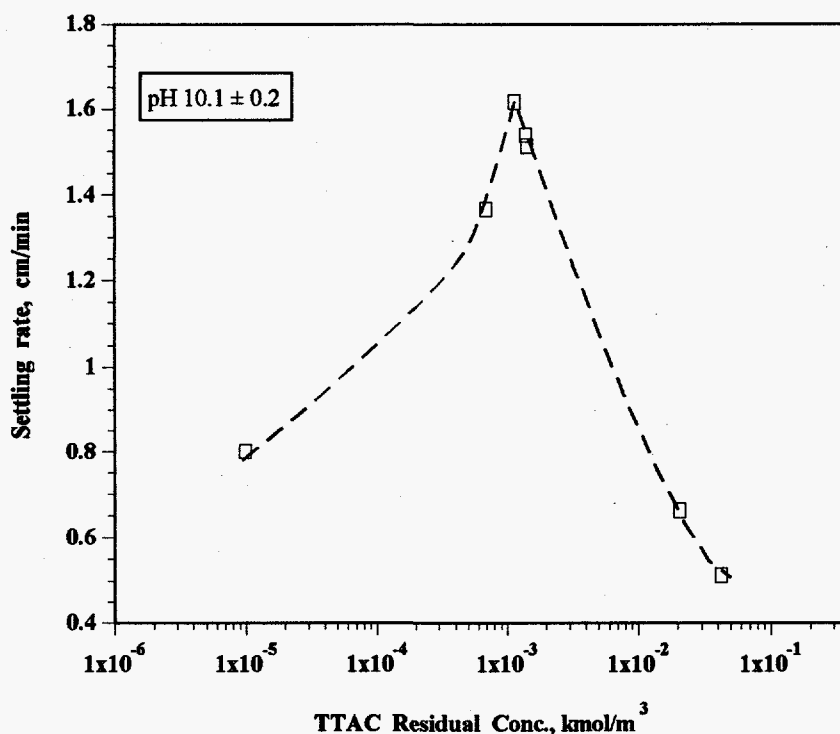


Figure 3 Settling rate of alumina suspensions after tetradecyl trimethyl ammonium chloride (TTAC) adsorption at pH 10.

With further increase in the TTAC adsorption, the settling rate decreases; this can be attributed to the increase of the positive charge of alumina at higher surfactant concentration (figure 2) causing repulsion between the alumina particles. As a result of the balance between the hydrophobic bridging force and the electrical repulsion force, the settling rate reaches a maximum at a concentration of about 1×10^{-3} kmol/m³. At higher concentrations the electrostatic forces

³P. Somasundaran, T.W. Healy and D.W. Fuerstenau, *J. Coll. Interf. Sci.*, **70**, 1966, 90.

dominates in this system and the settling rate decreases.

Changes in the microstructure of the adsorbed layer were probed using fluorescence spectroscopy. Pyrene monomer fluorescence is sensitive to the medium in which pyrene resides. In hydrophobic environments, the ratio of the intensities of the first and third peaks (I_3/I_1) on a pyrene emission spectrum is higher than when the pyrene is in a hydrophilic environment. The value for I_3/I_1 is 0.5-0.6 in water, 0.8-0.9 in surfactant micelles, and >1 in nonpolar solvents. Since this ratio can be used to characterize the polarity of environments, it is termed the *polarity parameter*.

The adsorption isotherm of TTAC on alumina is plotted in figure 4 along with changes in the polarity parameter of pyrene at the alumina-water interface and in the supernatant. It is observed that pyrene goes to the alumina-water interface in a narrow TTAC concentration range which corresponds to the sharp increase in adsorption isotherm. From this it is evident that pyrene is solubilized in TTAC aggregates at the alumina-water interface. However once TTAC micelles form in the supernatant, pyrene is preferentially solubilized into the micelles and does not go to the alumina-water interface in spite of the presence of TTAC hemimicelles. This result is interesting considering that in the alumina-SDS system, pyrene is preferentially solubilized in hemi-micelles at the alumina-water interface rather than SDS micelles in the supernatant⁴. It is proposed that aggregates of TTAC at the alumina-water interface are not as tightly packed. The solubilising power of the TTAC hemi-micelles at the alumina-water interface is not very high. The removal of the surfactant from the solid-liquid interface, a process of important consequence in enhanced oil recovery, depends upon the packing of the surfactant in the aggregates and on the strength of interaction between the surfactant and the solid. The role of the latter was investigated by diluting the suspensions and studying the desorption.

⁴P.Chandar, P. Somasundaran and N.J. Turro, *J.Coll. Interf. Sci.*, 117, 1987, 31.

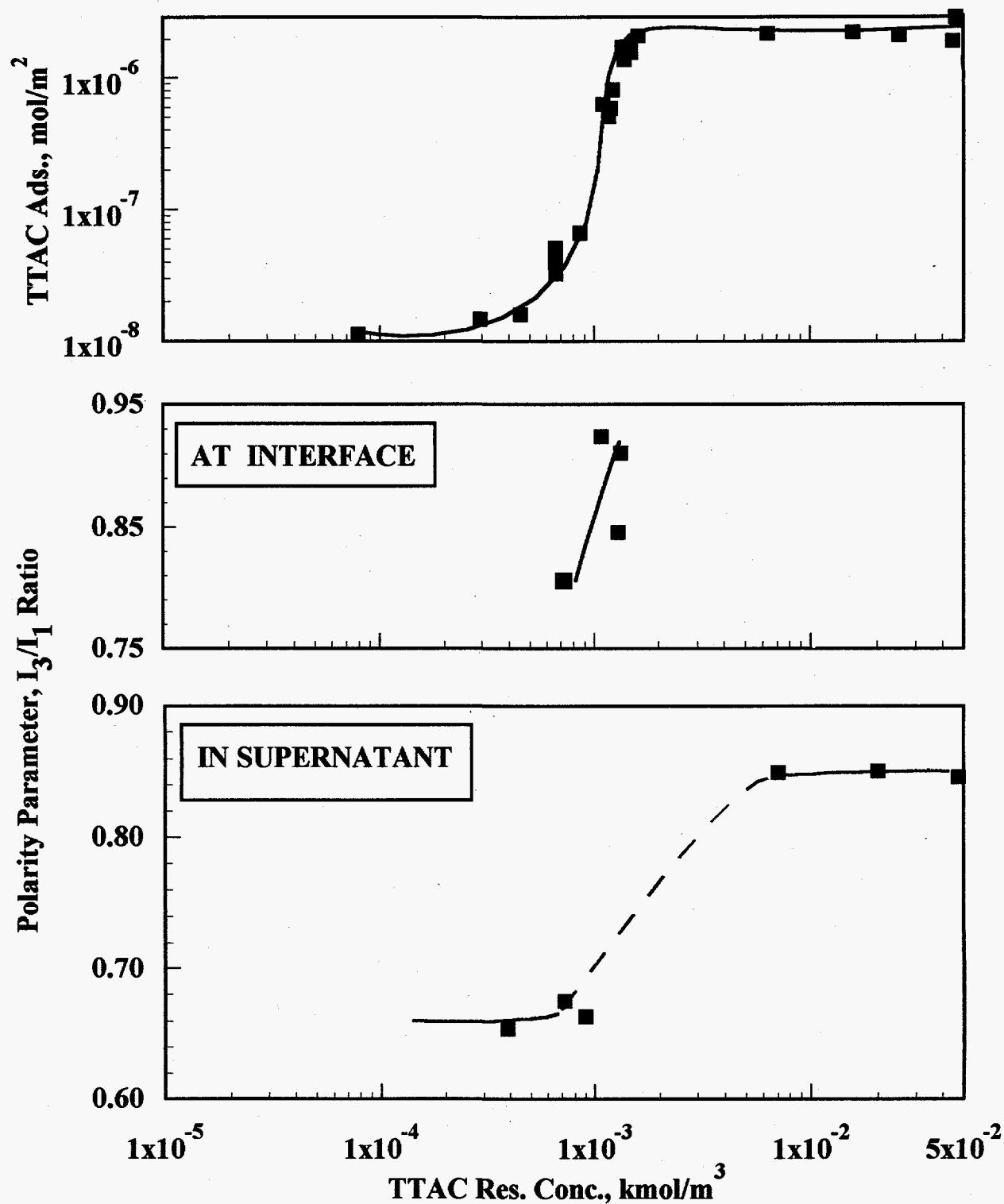


Figure 4 Adsorption isotherm of tetradecyl trimethylammonium chloride (TTAC) on alumina and corresponding changes in pyrene monomer fluorescence from the alumina water interface and the supernatant.

Desorption of cationic surfactant from alumina-water interface

The adsorption isotherm of tetradecyltrimethylammonium chloride (TTAC) on alumina was determined first and then supernatant solutions of different residual concentrations (C_r) along the isotherm were diluted with 0.03 kmol/m^3 sodium chloride solution and the slurry mixed for 15 hours. This procedure was repeated several times depending upon the concentration, and material balance has been done during the dilution. The results obtained are shown in figure 5. The solid line represents the initial adsorption isotherm. It is observed that adsorption is reversible in most cases, but interestingly it is irreversible in the low concentration range where significant changes in wettability normally occur. At low concentrations, there is some hysteresis with measurable differences in adsorption and desorption amounts.

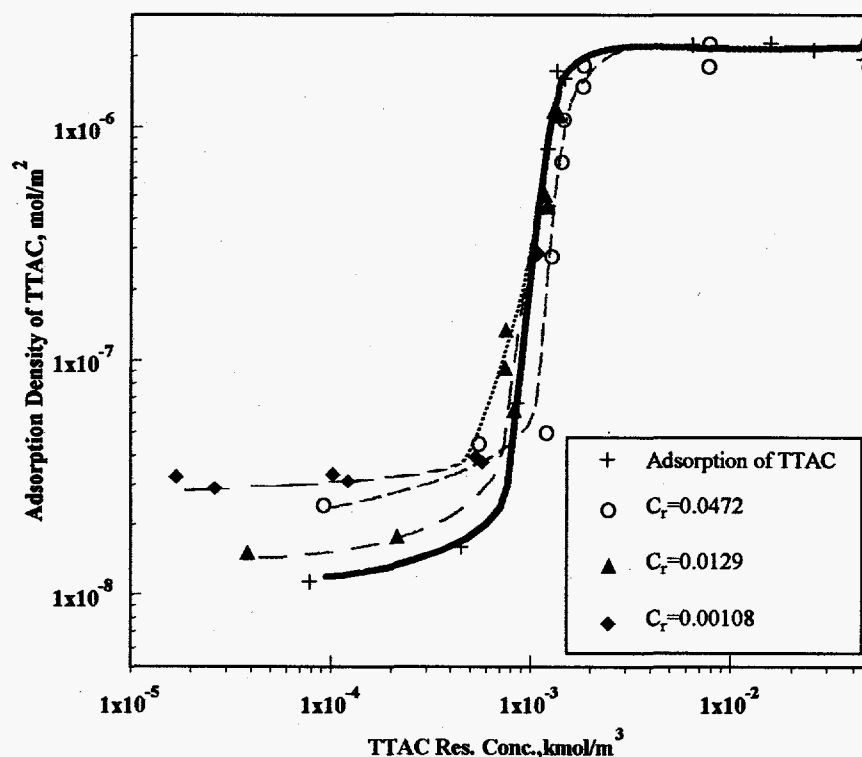


Figure 5 Desorption of TTAC from alumina upon dilution from different residual concentrations (C_r).

Fluorescence spectroscopy was used to probe changes in aggregation of surfactants at the solid-liquid interface upon dilution. Supernatant solutions of different residual concentrations along the isotherm were diluted with pyrene solutions at the desired ionic strength and the slurry conditioned for 15 h. The procedure was repeated several times. Pyrene emission spectra from the alumina-water interface were then obtained to gain an insight into the microstructural changes of the adsorbed layer upon dilution. The results are plotted in figure 6 along with the polarity parameter for pyrene dissolved in TTAC solutions of similar concentrations. Pyrene reports the presence of hydrophobic aggregates at the alumina-water interface. The value of the I_3/I_1 ratio decreases with decreases in concentrations but it is to be noted that hydrophobic aggregates are detected at concentrations lower than those at which they were first detected during adsorption (see figure 4). It should be mentioned that there will be some contribution to the spectrum by pyrene in the supernatant since a slurry was used in the sample cell. However for the residual concentrations discussed there will be no aggregates in solution as is clear from the results in figure 6. Aggregates form in solution only above a concentration of 1.5×10^{-3} kmol/m³. Thus the hydrophobic environment reported by pyrene must be from the interface.

The results obtained so far show that tetradecyltrimethylammonium chloride (TTAC) adsorbs strongly on alumina at pH 10 and dilution causes a rearrangement in the aggregate state at the alumina-water interface. Changes in this behavior in the presence of a cosurfactant were studied next using a mixture of a cationic surfactant and a nonionic surfactant. Moreover, surfactants used commercially are often present as mixtures, therefore a sustained effort is also necessary to understand the synergetic and competitive forces determining adsorption of surfactants from their mixtures.

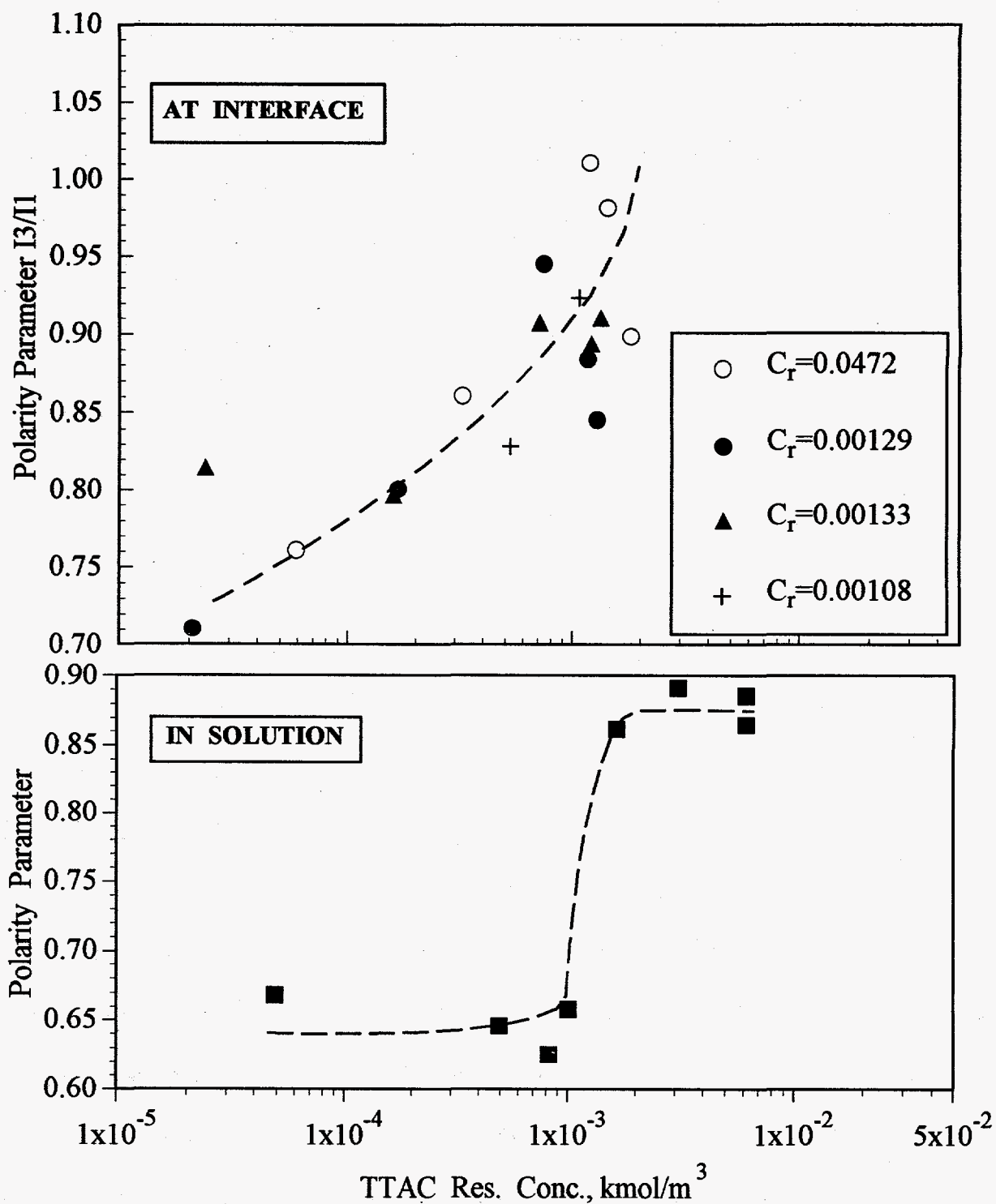


Figure 6 Changes in pyrene polarity parameter from the TTAC adsorbed layer on alumina upon dilution from different residual concentrations and also in bulk solution.

Adsorption of cationic-nonionic surfactant mixtures

Adsorption of tetradecyltrimethylammonium chloride (TTAC) and pentadecylethoxylated nonylphenol (NP-15) surfactant mixtures at the alumina-water interface was studied as a function of relevant variables. The experiments showed NP-15 not to adsorb by itself on alumina. In a study on the adsorption of polyethoxylated monolaurate (ML-n) and polyethoxyl lauryl ether (LE-n) on titania, Fukushima and Kumagai⁵ concluded that for adsorption on polar surfaces it is necessary that the nonionic surfactant have a radical which has sufficient adsorption force to overcome the strong interaction between water and the ethylene oxide groups. This observation is similar to our results on the adsorption of polyethylene oxide (PEO) on different minerals⁶. In this work we found PEO to adsorb on silica but not on alumina or hematite. It was proposed that for PEO to adsorb on oxide surfaces, the polymer has to displace enough water molecules bonded to the solid surface and create a strong entropic effect. In the case of the strongly hydrated alumina surface the polymer cannot displace sufficient water molecules necessary for adsorption of polymer. We propose similar reasons for the fact that NP-15 does not adsorb at the alumina-water interface.

Figure 7 shows the adsorption isotherms of pentadecylethoxylated nonylphenol with 15 ethylene oxide groups (NP-15) on alumina in the presence of pre-adsorbed TTAC and when added together with TTAC. In all these experiments the initial concentration of TTAC was fixed, and the pH was maintained at 10.

It is to be noted that tetradecyltrimethylammonium chloride does cause the adsorption of NP-15 on alumina. Pre-adsorbed TTAC functions as anchors for the adsorption of NP-15. With an

⁵S. Fukushima and S. Kumagai, *J. Coll. Interf. Sci.*, **42**, 1973, 539.

⁶E. Koksai, R. Ramachandran, P. Somasundaran and C. Maltesh, *Powder Tech.*, **62**, 1990, 253.

increase in TTAC addition, the adsorption of NP-15 increased with the adsorption isotherms shifting to lower NP-15 concentrations. It is also observed that above the TTAC concentration at which it forms hemimicelle at the alumina-water interface there is no further effect on the adsorption of NP-15.

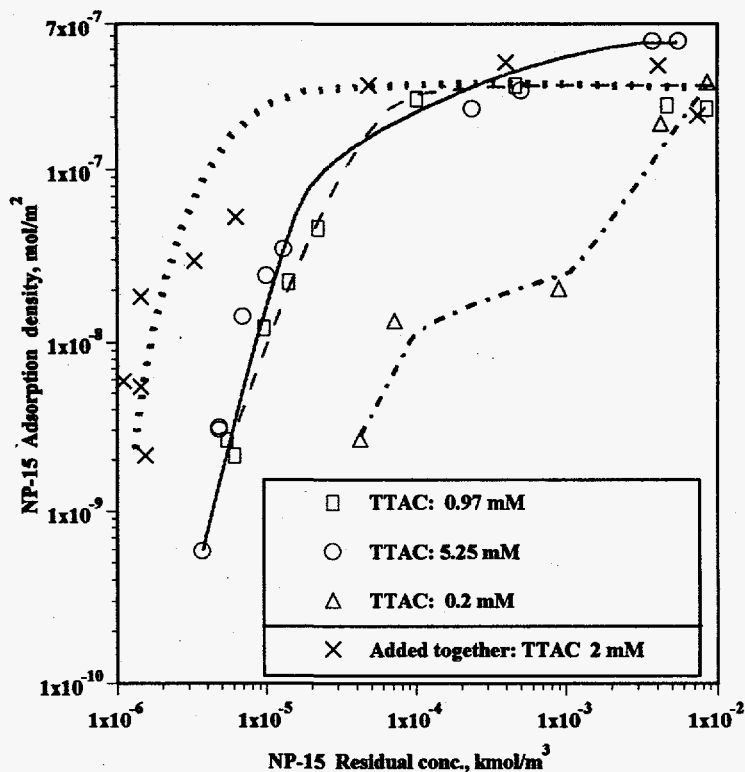


Figure 7 Adsorption isotherms of pentadecylethoxylated nonyl phenol (NP-15) on alumina: with preadsorbed amounts of tetradecyl trimethylammonium chloride (TTAC), and when added together with TTAC.

It is interesting to note the implication that TTAC hemimicelles are impermeable by the NP-15 even though there is synergism between the two species. It will be important to test this and investigate the reasons for this behavior. Desorption and reorientation of the surfactants adsorbed in the form of aggregates will depend to large extent on the activation barrier involved in dehemimicellisation.

The results also show that the order of addition of the surfactants has a marked effect on the

adsorption of NP-15. If NP-15 and TTAC were pre-mixed and added to the alumina suspension together, the adsorption density of NP-15 is higher in the low concentration range. This indicates that NP-15 adsorption with TTAC is not completely reversible, but is controlled by the nature of molecules packed at the alumina-water interface. Particle wettability and dispersion can also be expected to be affected by this markedly. It is important to note the lack of adsorption of the nonionic polyethoxylated nonyl phenol (NP-15) without the synergistic interaction of the cationic TTAC which shows the essential role of the electrostatic interaction in initiating the adsorption.

Since it is seen that the adsorption of the pentadecylethoxylated nonylphenol (NP-15) from its mixtures with tetradecyl trimethyl ammonium chloride (TTAC) is higher than when TTAC was preadsorbed, adsorption from mixtures with different TTAC:NP-15 ratios was studied. Total adsorption as well as adsorption of the components are given in figures 8 through 10. In all the experiments tetradecyltrimethylammonium chloride (TTAC) and pentadecylethoxylated nonylphenol (NP-15) were pre-mixed in 0.03 M sodium chloride solution and mixed with Linde A alumina for 15 hours at pH 10 under which conditions the alumina surface is originally negatively charged. Results reported in this project have shown that the adsorption of TTAC on alumina is higher at pH 10 than at lower pH values. Figure 8 shows the adsorption isotherms of TTAC in the presence of different amounts of NP-15. Zeta potential of alumina particles after adsorption under the above conditions are given in figure 11.

With the addition of the NP-15, TTAC adsorption rises in the low concentration range due to earlier onset of hemi-micelle aggregation for both 4:1 and 1:1 TTAC:NP-15 ratios. For the 1:4 ratio no such trend is clear in the concentration range studied. At high concentrations, adsorption density decreases markedly with the addition of the nonionic surfactant. This is attributed to the

competitive adsorption provided by NP-15. To quantitatively derive the adsorption mechanism governing the individual adsorptions, it is necessary to determine the variation in the monomer concentration of each component in the system. Ultrafiltration will be tested to determine such monomer concentrations in subsequent work.

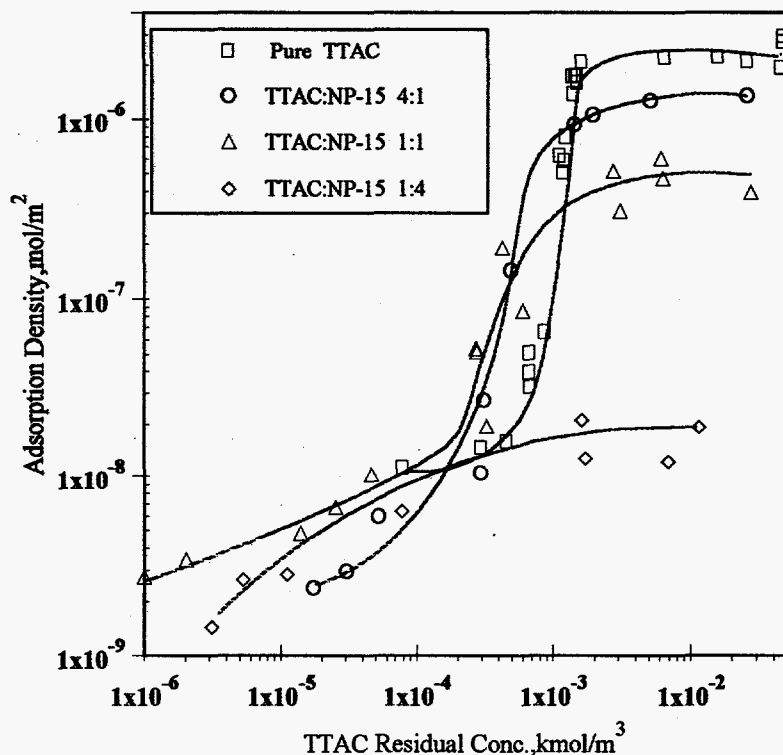


Figure 8 Adsorption of tetradecyl trimethyl ammonium chloride (TTAC) in the presence and absence of NP-15.

With respect to the adsorption of nonionic NP-15 from the mixed system, while the nonionic surfactant NP-15 does not adsorb by itself on alumina, significant adsorption of the NP-15 occurs even at a ratio of 1:4 TTAC:NP-15.

With an increase in TTAC ratio in the mixtures, the adsorption of NP-15 is further enhanced significantly, and the adsorption isotherms are shifted to the lower concentration range. The residual surfactant concentration at which maximum (or plateau) adsorption density is attained usually

corresponds to the critical micelle concentration (CMC) of the surfactant. The isotherm normally shifts to lower concentrations if the CMC and hemimicelle concentration (HMC) of the surfactant decrease. But in the present system, the onset of the plateau of the adsorption isotherm of NP-15 from mixtures with TTAC does not correspond to the CMC of the mixtures.

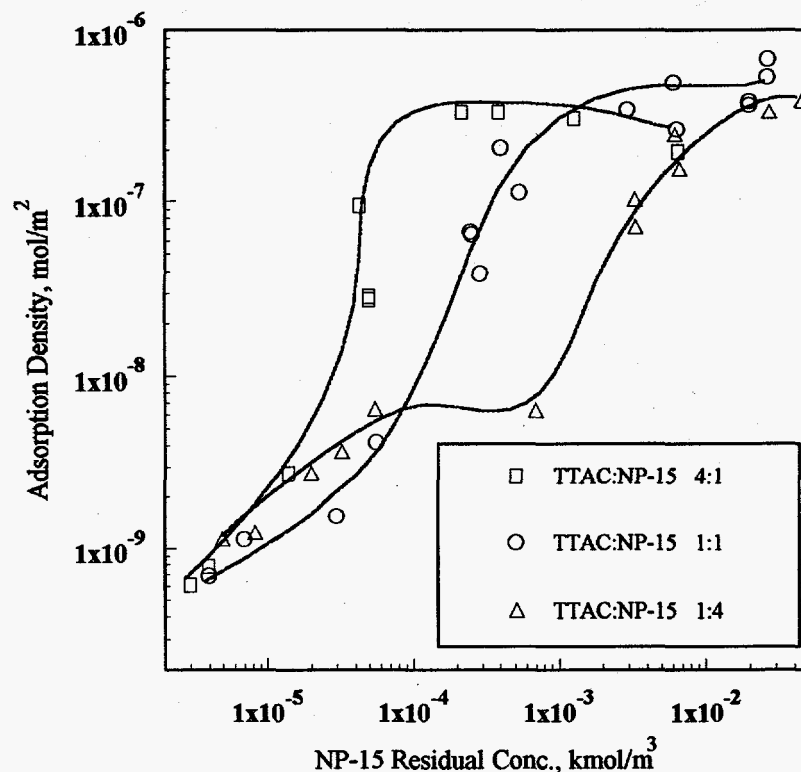


Figure 9 Adsorption of pentadecylethoxylated nonylphenol (NP-15) on alumina in presence of varying amounts of tetradecyltrimethylammonium chloride (TTAC).

For example, the CMC of the 4:1 mixture solution is the highest of all mixtures (see figure 13), but the isotherm of NP-15 from this mixture is located in the lowest concentration range. This implies that the adsorption of NP-15 is controlled not by the micelle formation alone, but also by the adsorption of TTAC, the change in monomer composition and the structure of adsorbed layer. All these factors warrant further investigation in order to understand the mechanism and to develop the capability to manipulate the adsorption behavior of mixtures.

The peculiar S-shape isotherm obtained for NP-15 adsorption as a function of NP-15 residual concentration should be noted and is in agreement with our previous work⁷. This is attributed to the more effective coadsorption of NP-15 inside the aggregates as the number of TTAC hemimicelles at the alumina-water interface increases. It is to be noted that the residual concentration of tetradecyl trimethylammonium chloride (TTAC) varies from point to point along the NP-15 adsorption isotherm.

The total adsorption density of tetradecyltrimethylammonium chloride (TTAC) and pentadecylethoxylated nonylphenol (NP-15) on alumina are plotted in figure 10 as a function of total surfactant concentration. It can be seen that with an increase in NP-15 in the mixtures the total adsorption density in moles/m² decreases and this is suggested to be due to large size of NP-15 and the steric hinderance caused by it.

Since the NP-15 molecules are much larger than the TTAC molecules, the adsorbed NP-15 will occupy more area thus reducing the area available for TTAC. Another plausible reason is the alteration in the structures of hemimicelles and micelles in the system with some screening of TTAC charge by the NP-15 with the increase of NP-15 in the mixtures. This will reduce the net electrostatic attractive forces between the alumina surface and the TTAC molecules which in turn can decrease also the adsorption of NP-15, since the adsorption of NP-15 depends upon the coadsorbed TTAC for anchoring.

⁷P. Somasundaran, Edward Fu and Qun Xu, *Langmuir*, **8**, 1992, 1065.

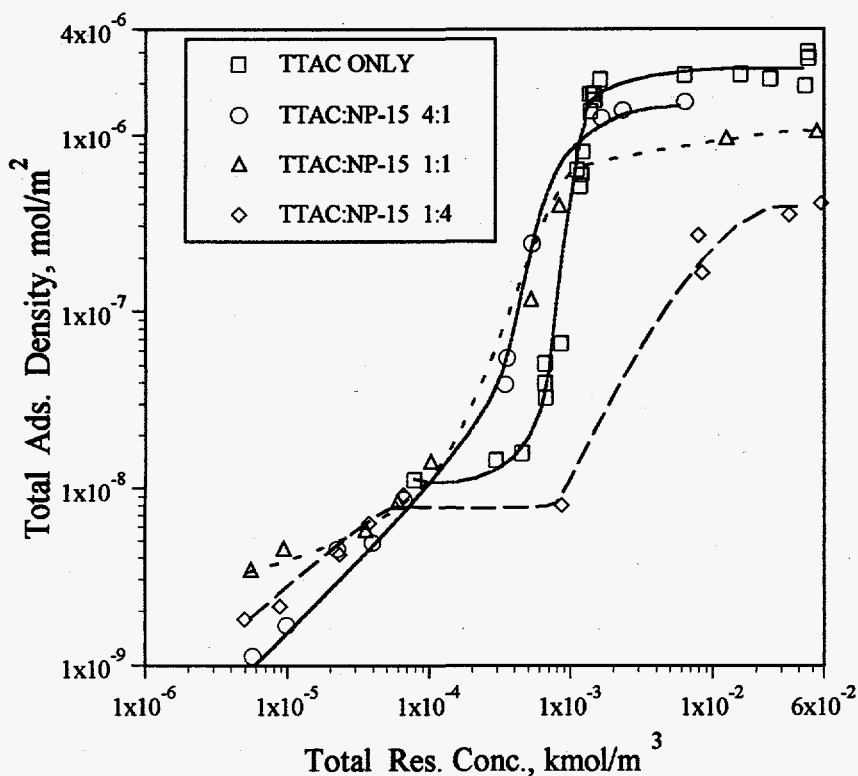


Figure 10 Total adsorption of surfactant mixtures at the alumina-water interface.

This hypothesis was tested by studying the zeta potential change due to adsorption and the results obtained are shown in figure 11. In this system, the zeta potential of alumina particles is decided mainly by the adsorption of the oppositely charged TTAC. From figure 11 it can be seen that with an increase of NP-15 in the mixture, the zeta potential of alumina decreases drastically, especially in the high concentration range. This is in agreement with the adsorption isotherms of TTAC and NP-15 in figures 8 & 9 respectively. Comparing the isoelectric point (IEP) for alumina in the presence of mixtures to that in the presence of TTAC alone it can be seen that with an increase in the NP-15 the IEP is shifted to higher TTAC concentrations. Upon examining the adsorption density of TTAC at IEP, it can be seen that the adsorption density of TTAC in mixtures is higher than that for TTAC alone. This means that the effect of TTAC in mixtures on zeta potential reduction is

less than that of TTAC when present alone. It can be concluded that the positive charge of the TTAC ionic head is partially screened by the co-adsorbed nonionic NP-15 molecule. Any effect of structure of the adsorbed layer on the position of the shear plane and possible effects on it is also to be determined and taken into account.

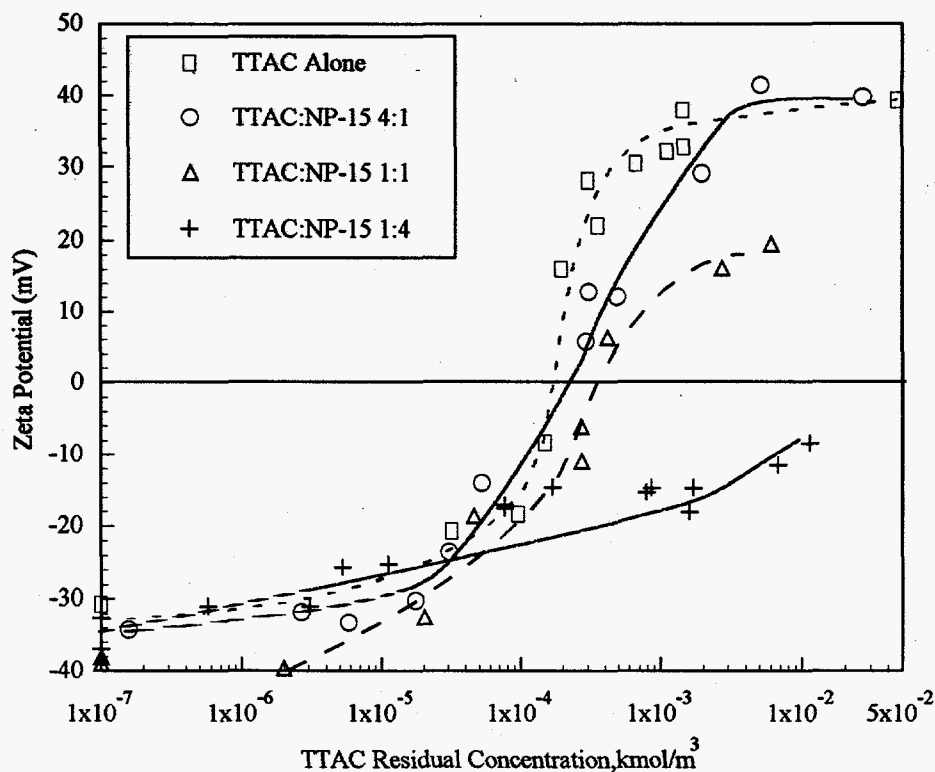


Figure 11 Zeta-potential of alumina after adsorption of TTA:NP-15 mixtures of different composition.

It will be useful to examine the ratio of adsorption densities of TTAC to NP-15 as a function of total residual concentration. Such a plot is given in figure 12. The shapes of the ratio vs curves change drastically with the cationic/nonionic surfactant ratio exhibiting an intriguing set of interactions between the two components and suggesting ways to probe them. It can be seen that the ability of the two surfactants to cooperate/compete at the alumina-water interface changes over the entire concentration range. This suggests the monomer compositions and adsorption mechanism to

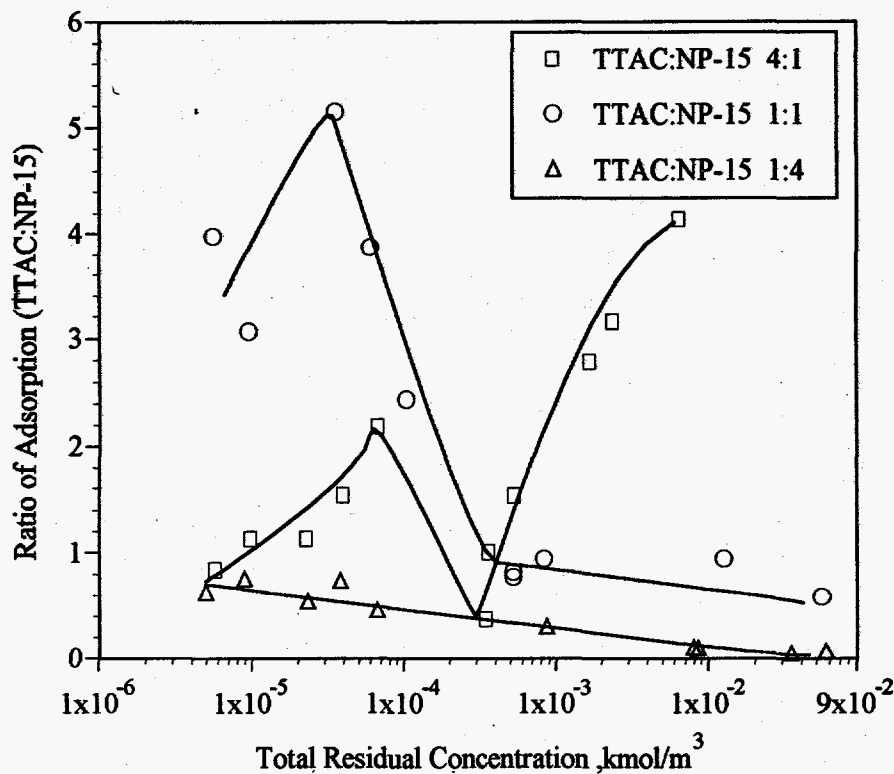


Figure 12 Ratio of adsorption densities of TTAC:NP-15 for different surfactant mixtures.

be changing over the concentration range studied. Clearly it becomes interesting to investigate these issues and develop a model that determines adsorption of both components as a function of their activities in solution and synergies/competitions involved.

Surface tension of different mixtures was measured before and after adsorption to investigate the partitioning of the two surfactants to the alumina-water interface and the results obtained are shown in figures 13 and 14. Surface activity of the nonionic NP-15 is greater than that of the TTAC, and the total activity decreases with an increase of TTAC in the mixtures. Comparison of results in figure 13 to those in figure 14 shows that there is not much change in the surface tension behavior due to adsorption. Any change should correspond to the relative adsorption of the two surfactants.

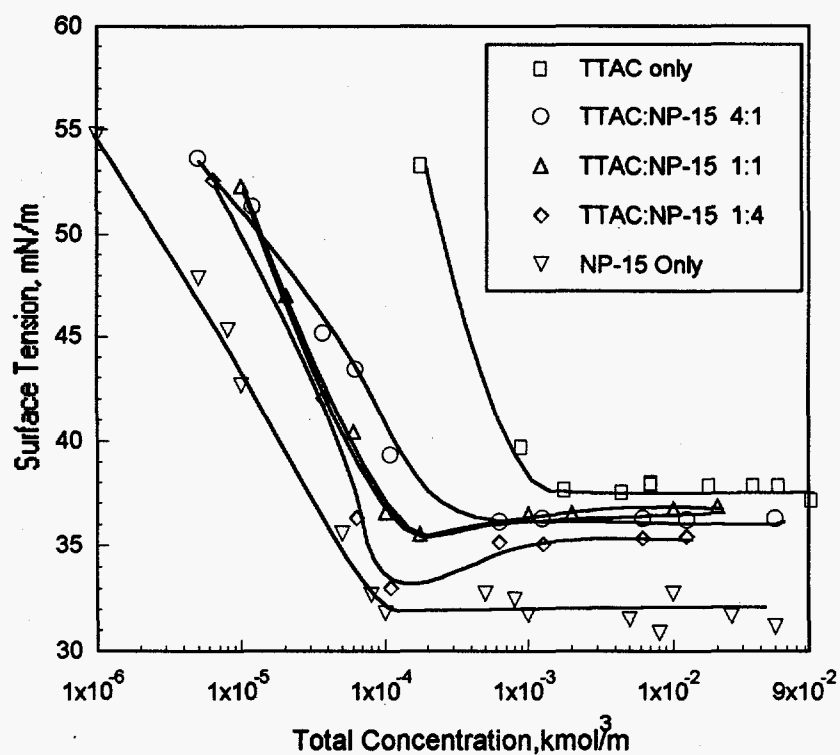


Figure 14 Surface tension of solutions of TTAC, NP-15 and their mixtures.

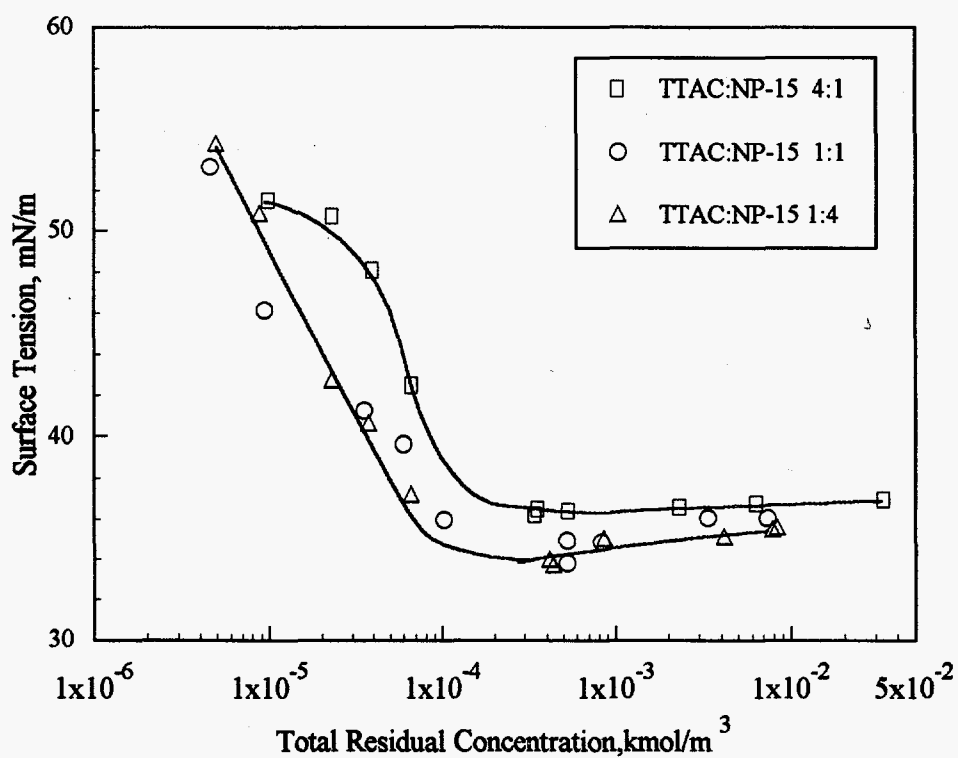


Figure 13 Surface tension of TTAC:NP-15 surfactant mixtures after adsorption.

If TTAC adsorbs more than NP-15 (compared to the ratio in the initial mixture) surface activity of the mixed solution can be expected to increase, whereas, if NP-15 adsorbs more, surface activity can decrease. For example, in the 4:1 mixed system the NP-15 adsorbed significantly in the low concentration range, and this caused the surface tension to shift to higher values in the same concentration range.

It has been shown very clearly in this work that interactions between the two surface active components in a mixture can lead to drastic alterations in the adsorption behavior of the system reinforcing the need to understand such behavior since, as mentioned earlier, surfactant systems used in practice are invariably of the mixed type. It is important to investigate the microstructure of the adsorbed layer and changes in it as well as to elucidate the effects of the mechanisms involved and the variation in the adsorption process on interfacial properties such as wettability.

Theoretical and Thermodynamic Modelling of Cationic - Nonionic Surfactant Interactions

In an attempt to interpret adsorption and desorption behavior of mixed surfactant systems, regular solution theory was used to model the interactions between tetradecyltrimethylammonium chloride (TTAC) and pentadecylethoxylated nonylphenol (NP-15). The interaction parameter β and the monomer concentrations were calculated for different mixtures.

Solution behavior of surfactant mixtures

Based on a pseudophase separation model, Rubingh and Holland^{8,9} have utilized the regular solution theory to treat mixed surfactant systems. For surfactant mixing, changes in the charged state

⁸D.N. Rubingh, in Solution Chemistry of Surfactants, K.L. Mittal (ed), Vol 1, Plenum Press, New York, 337.

⁹P.M. Holland and D.N. Rubingh, *J. Phys. Chem.*, **87**, 1983, p 1984.

of mixed micelles containing ionic surfactants (ionic/nonionic, and cationic/anionic mixed micelles) can be included in the activity coefficients in the micelles. These activity coefficients f_i for binary mixtures can be expressed by the following equations:

$$f_1 = \exp [\beta \cdot (1 - x)^2] \quad (1)$$

$$f_2 = \exp [\beta \cdot x^2] \quad (2)$$

where x is the mole fraction of surfactant 1 in mixed micelles. β is a measure of the deviation of the mixture from ideality and is related to the molecular interactions between surfactants 1 and 2 in the surface phase and is defined as follows:

$$\beta = \left[\frac{N_A (w_{11} + w_{22} - 2w_{12})}{RT} \right] \quad (3)$$

where w_{11} and w_{22} are the energies of interaction between similar kinds of surfactant molecules in the single component micelles; w_{12} is the interaction energy between different kinds of molecules in the mixed micelles; and N_A is the Avogadro number. The interaction parameter β can be evaluated as an experimental parameter from CMC values and used to interpret subsequent experiments. The following equations permit solution for β in terms of C_1, C_2 and C^* :

$$\left[\frac{x^2 \ln \left(\frac{C^* \alpha}{C_1 x} \right)}{(1 - x)^2 \ln \left(\frac{C^* (1 - \alpha)}{C_2 (1 - x)} \right)} \right] = 1 \quad (4)$$

$$\beta = \left[\frac{\ln \left(\frac{C^* \alpha}{C_1 x} \right)}{(1-x)^2} \right] \quad (5)$$

Where α is the mole fraction of surfactant 1 in the total mixed solute, C^* is the CMC of the mixture and C_1 & C_2 are the CMCs of the individual surfactants 1 and 2. If one measures the CMC of a binary mixed surfactant, C^* , as a function of the mole fraction in bulk, α , and C_1 and C_2 , then one can determine x and C^* by means of Eq. (4) and (5). The concentrations of the monomers in the mixture can be calculated using the following equations:

$$C_1^m = \left[\frac{- (C - \Delta) + [(C - \Delta)^2 + 4\alpha C \Delta]^{1/2}}{2 \cdot (f_2 C_2 / f_1 C_1 - 1)} \right] \quad (6)$$

where $(\Delta = f_2 C_2 - f_1 C_1)$

$$C_2^m = \left(1 - \frac{C_1^m}{f_1 C_1} \right) \cdot f_2 C_2 \quad (7)$$

Although the regular solution theory has been criticized by some researchers, it has provided a very tractable way to describe the behavior of mixed surfactant aggregates. The calculated results of x and C^* are shown in Table I.

Table I **Calculated results of x and C^* by regular solution theory**

α	$\beta = - 1.5$		$\beta = - 1.0$	
	x	C*(10 ⁻⁴ M)	x	C*(10 ⁻⁴ M)
0.05	0.4374	5.33	0.4271	6.03
0.10	0.5439	3.90	0.5512	4.42
0.125	0.5795	3.49	0.5925	3.93
0.20	0.6567	2.69	0.6808	3.01
0.25	0.6974	2.37	0.7232	2.63
0.30	0.7267	2.12	0.7580	2.34
0.40	0.7793	1.78	0.8135	1.92
0.50	0.8229	1.54	0.8571	1.65
0.60	0.8613	1.37	0.8932	1.44
0.70	0.8968	1.24	0.9244	1.29
0.80	0.9308	1.13	0.9520	1.16
0.90	0.9647	1.05	0.9770	1.06
0.95	0.9821	1.01	0.9887	1.02
0.99	0.9964	0.99	0.9978	0.99

Critical micelle concentrations of the mixtures determined by the surface tension measurement are plotted in figure 15 as a function of NP-15 mole fraction. Regular solution theory has been used to fit these data.

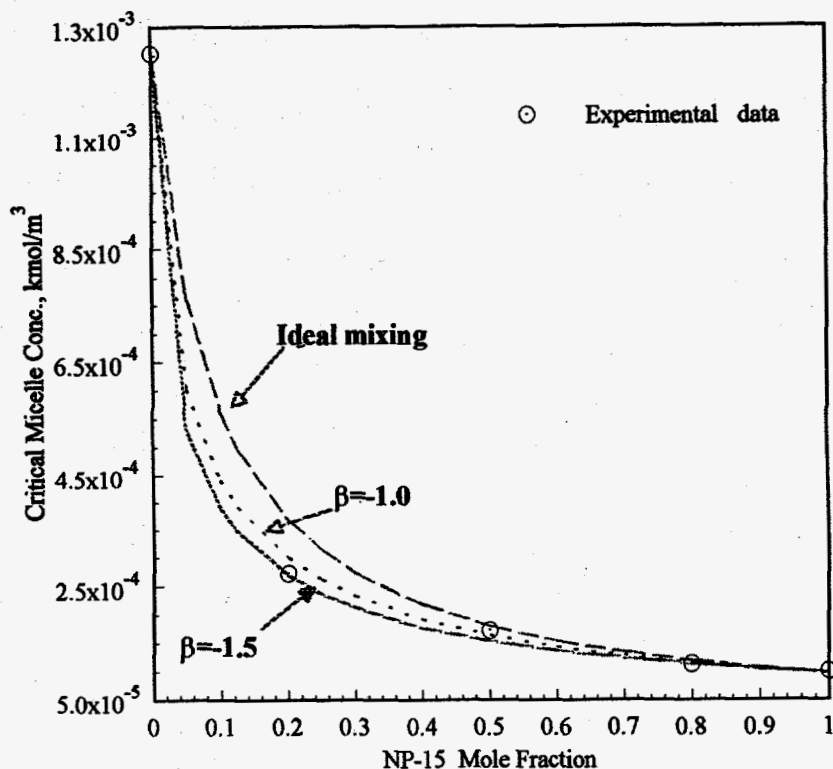


Figure 15 Regular solution and ideal mixing theory for determining the interaction parameter for the tetradecyl trimethylammoniumchloride (TTAC) pentadecylethoxylated nonyl phenol (NP-15) system.

It was found that the interaction parameter β for this system is between -1.5 and -1.2. A considerable number of binary mixed micellar systems have been studied using regular solution theory. Generally, the strength of interaction in mixed systems with cationic surfactants increases in the order of cationic-cationic, cationic-zwitterionic, cationic-nonionic, and cationic-anionic. For cationic-anionic system the value of the interaction parameter β can be about -25, for cationic-nonionic, -4.6 to -1.0, for cationic-cationic, about -0.2 to 0. In addition to the nature of the components in the mixture, the interaction parameter is affected by the structure of the surfactants and the ionic strength of the mixed system. The interaction parameter observed for the TTAC:NP-15 system is not very large. This indicates that the interaction between TTAC and NP-15 in 0.03 M NaCl solution is not very strong.

To better understand the adsorption/desorption mechanisms the monomer concentrations of different mixtures in this system were calculated using the regular solution theory with an interaction parameter of -1.5. The results obtained are shown in figures 16 and 17.

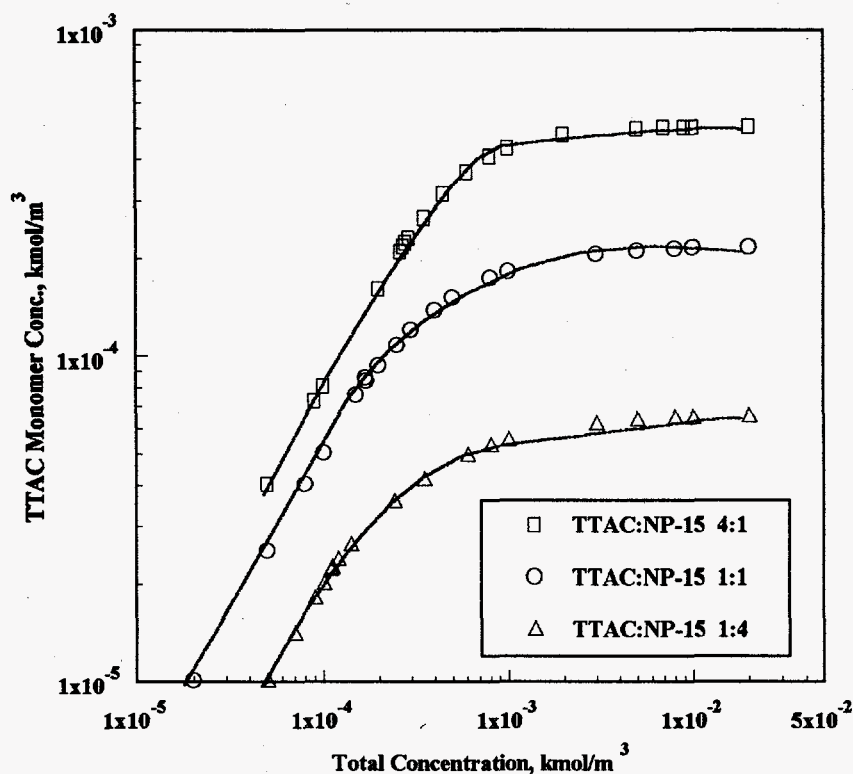


Figure 16 Monomer concentrations of tetradecyl trimethylammoniumchloride (TTAC) in mixtures with pentadecylethoxylated nonyl phenol (NP-15) calculated using regular solution theory with an interaction parameter -1.5

Comparing these monomer concentrations with the adsorption isotherms (figures 8 and 9) it can be found that the adsorption of NP-15 does not depend upon its monomer concentration in the mixtures. For example, the adsorption of NP-15 in 4:1 TTAC:NP-15 mixture is the most significant in all these mixtures, but its monomer concentration is the lowest. This result is in agreement with the fact that the adsorption of NP-15 depends on the pre-adsorbed TTAC acting as anchors. For the adsorption of TTAC, the adsorbed amount corresponds to the monomer concentrations in the mixtures. The higher the monomer concentration, the higher is the adsorption density.

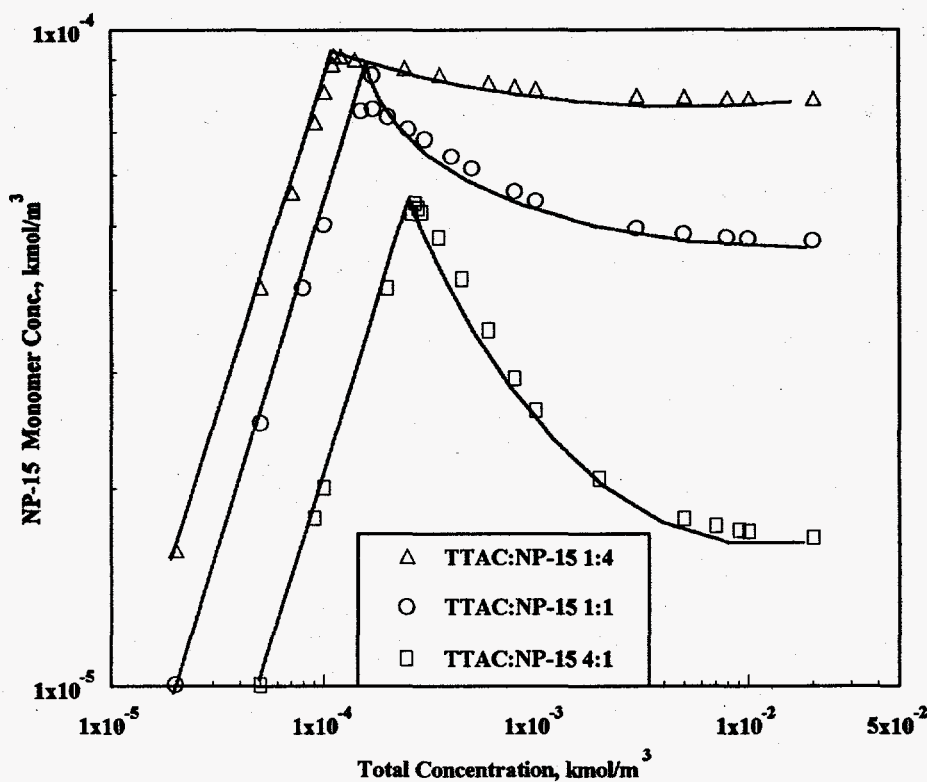


Figure 17 Monomer concentrations of pentadecyloxyated nonyl phenol (NP-15) in mixtures with tetradecyl trimethylammonium chloride (TTAC) calculated using regular solution theory with an interaction parameter = -1.5.

Since these monomer concentrations are the concentrations calculated before adsorption, it is not directly related to changes in the monomer composition upon adsorption and during desorption. It is therefore necessary to determine the variation of the monomer concentration of each component during the adsorption and desorption directly by some suitable experimental methods and we are pursuing this aspect now.

Whereas adsorption of TTAC is greatly affected by the presence of NP-15 the adsorption of the latter depends solely upon the presence of TTAC, we suspect the aggregate size and structure to be affected and this in turn should also control the desorption process. It remained to be seen how changes in the aggregate structure would affect desorption.

Desorption of surfactant mixtures from alumina-water interface

Interactions between surfactants and solids can be understood better by studying desorption along with adsorption. It has been shown earlier that the desorption of tetradecyl trimethyl ammonium chloride (TTAC) from alumina-water interface was reversible at high concentrations but was irreversible at lower concentrations. This was attributed to changes in the structure of the adsorbed layer upon dilution. Similar studies were conducted next with the mixed adsorbed layer.

The desorption tests consisted of mixing of supernatants of slurries from adsorption tests for 15 hours with the desired amounts of diluents adjusted for pH and ionic strength. This procedure was repeated several times. The results obtained for the desorption of a 4:1 TTAC:NP-15 mixture are shown in figures 18 & 19. It is noted that the desorption of TTAC from a 4:1 mixture (figure 18) is

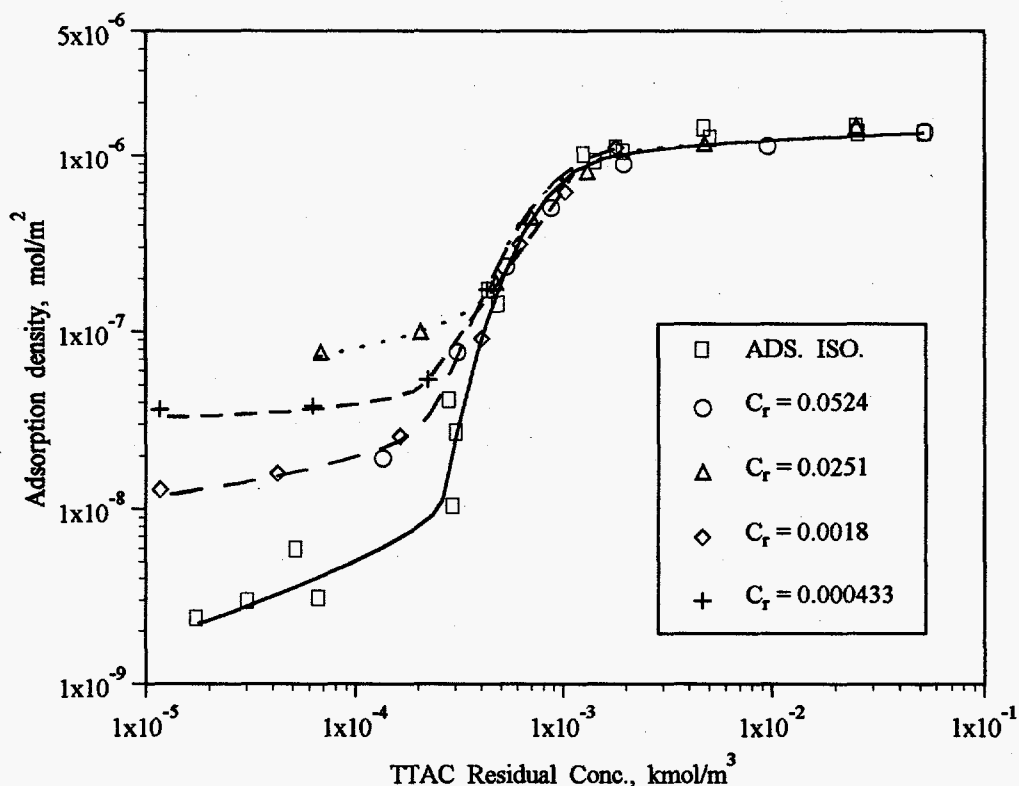


Figure 18 Desorption of tetradecyl trimethyl ammonium chloride (TTAC) from mixed adsorbed layer on alumina upon dilution from different residual concentrations of TTAC (C_r). TTAC:NP-15 = 4:1

similar to that for TTAC alone (figure 5).

At high concentrations the adsorption of TTAC is reversible, but at low concentrations the desorption shows some positive hysteresis, i.e. at same residual concentrations, the adsorption density is higher after desorption than that after adsorption. This is attributed to the hysteresis involved in the deaggregation of the hemimicelles from the interface. Interestingly, the fully grown hemimicelles come off the surface easily upon dilution whereas the incipient ones do not. Similar isotherms for the desorption of NP-15 is shown in figure 19. As reported earlier, the adsorption of NP-15 on alumina requires the tetradecyl trimethyl ammonium chloride (TTAC) to coadsorb and act as an anchor. It is the reasonable to expect the desorption behavior of the NP-15 to be controlled by the desorption of TTAC.

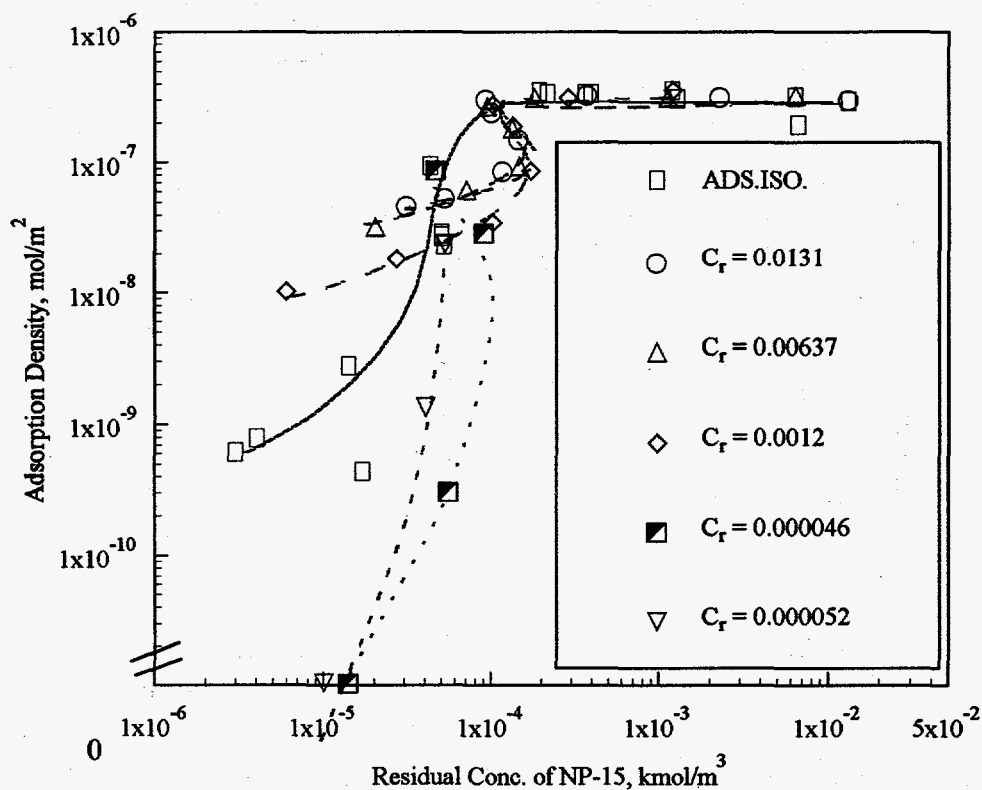


Figure 19 Desorption of pentadecyl ethoxylated nonyl phenol (NP-15) from alumina upon dilution from different residual concentrations (C_r). TTAC:NP-15 ratio = 4:1.

At high concentrations the adsorption density of TTAC does not change much upon dilution, neither does NP-15 desorb from the interface under these conditions. However in cases where TTAC desorbs from the interface, desorption of NP-15 is significant and S-shape desorption isotherms are obtained. The desorption of NP-15 is facilitated in this case by the desorption of TTAC. For dilutions from high concentrations, the desorption of NP-15 shows some positive hysteresis (similar to the positive hysteresis of TTAC) but only when the residual concentration becomes low due to dilution.

The desorption isotherms for a 1:1 TTAC:NP-15 mixture are shown in figures 20 & 21. It can be seen that at this ratio both TTAC and NP-15 desorb significantly and the desorption isotherms show negative hysteresis, i.e. the surfactant adsorption at the interface is less during desorption than that during adsorption at the same residual concentration.

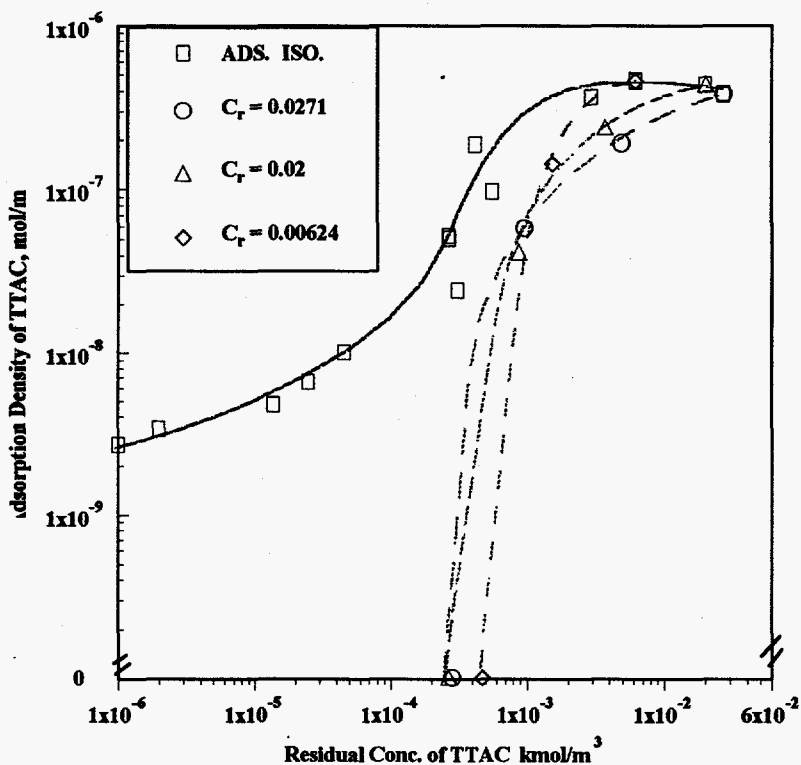


Figure 20 Desorption of tetradecyl trimethylammonium chloride (TTAC) from alumina-water interface upon dilution from different residual concentrations (C_r) in presence of 1:1 pentadecyl ethoxylated nonyl phenol (NP-15).

As the NP-15 content of the mixture increases, the positively charged head of the TTAC will be partially shielded from each other by the co-adsorbed nonionic NP-15 molecules. This will decrease the electrostatic interaction between the cationic TTAC molecules and the negatively charged alumina surface and facilitate desorption.

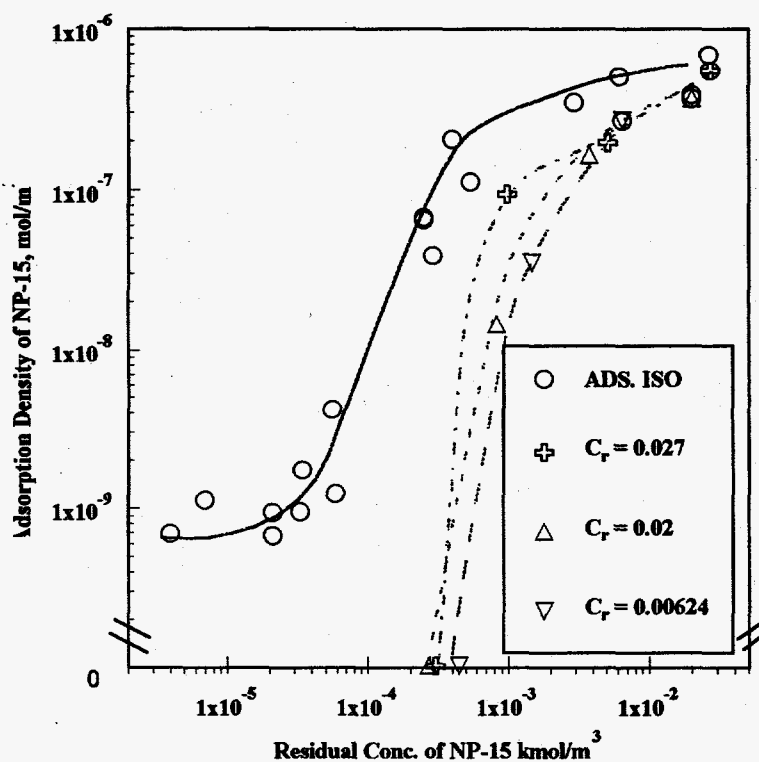


Figure 21 Desorption of pentadecylethoxylated nonyl phenol (NP-15) upon dilution from different residual concentrations (C_r) in presence of 1:1 tetradecyl trimethylammonium chloride (TTAC).

The desorption of 1:4 TTAC:NP-15 mixed system is shown in figures 22 & 23. At this ratio the adsorption of TTAC is very low. Nevertheless, the desorption of TTAC in this system still shows some negative hysteresis. The desorption of NP-15 shows some positive hysteresis. The mechanisms of desorption in this mixed system are evidently complex and merit further investigation.

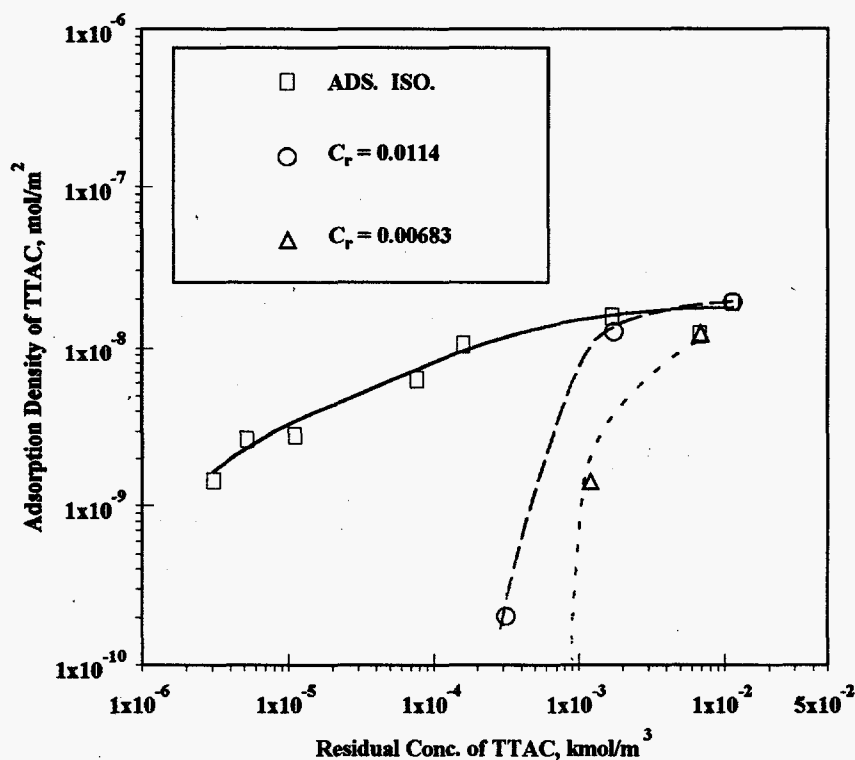


Figure 22 Desorption of tetradecyl trimethyl ammonium chloride (TTAC) from alumina upon dilution from different residual concentrations (C_r). TTAC:NP-15 ratio = 1:4.

From the above results it is evident that the desorption behavior of this mixed system depends upon the ratio of surfactants in the mixture. With an increase of NP-15 in the mixture the desorption of TTAC becomes easy. The desorption of both surfactants show significant negative hysteresis at a ratio of 1:1. Further study is needed to understand the precise relationship among desorption behavior, structure of the adsorbed layers, mixed micelles and changes in the monomer concentration ratio during desorption.

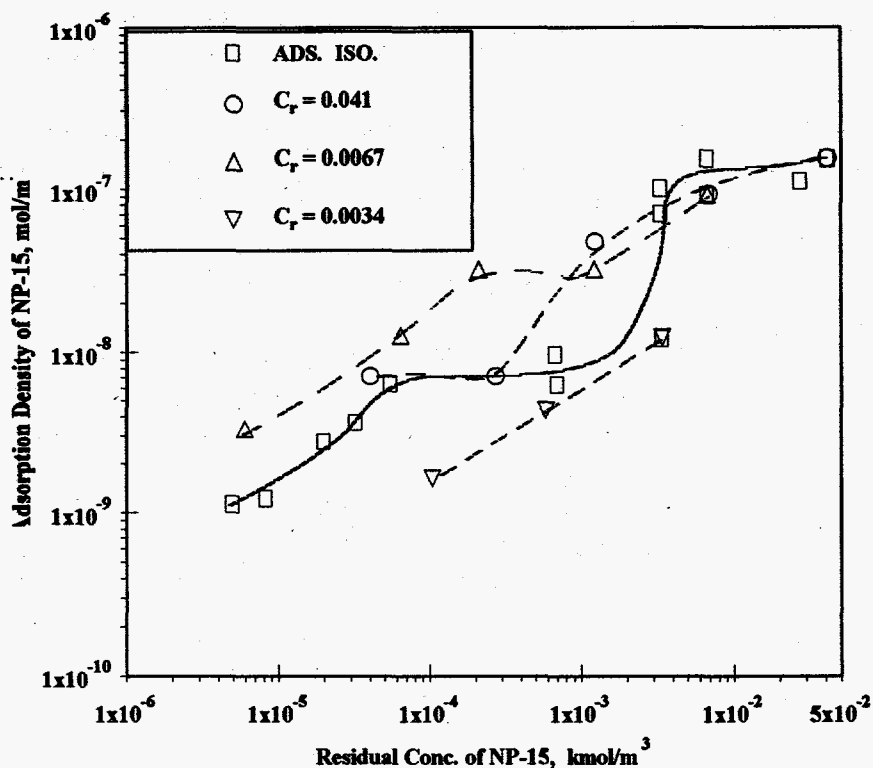


Figure 23 Desorption of pentadecyl ethoxylated nonyl phenol (NP-15) from alumina upon dilution from different residual concentrations (C_r). TTAC:NP-15 ratio = 1:4.

It is shown that the interactions between surfactant mixtures can be exploited to control and alter the adsorption and desorption behavior of the individual surfactants. Thermodynamic models can be used to calculate the monomer concentrations and predict adsorption behavior but only if the adsorption is not contingent upon the adsorption of a coadsorbing species. Future work will concentrate on determining the monomer concentrations existing under the experimental conditions using such techniques as ultrafiltration. Fluorescence and spin resonance spectroscopy will be used to probe the adsorbed layer and determine aggregation number, microviscosity, etc. in mixed surfactants during adsorption and desorption.

Sodium dodecyl sulfate (SDS)/Octaethyleneglycol mono-n-alkyl ether (C_nEO_8) mixture adsorption

During the first year, studies on interactions between anionic and nonionic surfactants were conducted and the effect of the surfactant structure on the adsorption of single surfactants was determined. During the current year, effect of surfactant structure in controlling mixture adsorption was studied. Effect of hydrocarbon chain length of octaethylene glycol mono n-decyl ether (C_nEO_8) type nonionic surfactants on the adsorption of 1:1 mixtures of sodium dodecyl sulfate (SDS)/(C_nEO_8) at the kaolinite/water interface was studied. Changes in aggregate size was also investigated using fluorescence spectroscopy.

Results reported during the preceding year indicated that with increase in hydrocarbon chain length of the nonionic surfactant C_nEO_8 ($n=10,12,14,16$) the adsorption on kaolinite increased but there was only partial coverage of the kaolinite surface (surface coverage Θ varied from 0.11 to 0.19). The adsorption of 1:1 mixtures of sodium dodecyl sulfate (SDS) and octaethylene glycol mono n-alkyl ether (C_nEO_8) mixtures at the kaolinite-water interface was studied in detail first this year and the results are given in figure 24. It is noted that the isotherms for the adsorption of SDS are identical to each other when the hydrocarbon chain length of the nonionic surfactants, octaethylene glycol mono n-alkyl ethers ($C_{12}EO_8$, $C_{14}EO_8$, $C_{16}EO_8$), is equal to or longer than that of the anionic SDS (C_{12}), but markedly different from that of the isotherm in the absence of the C_nEO_8 .

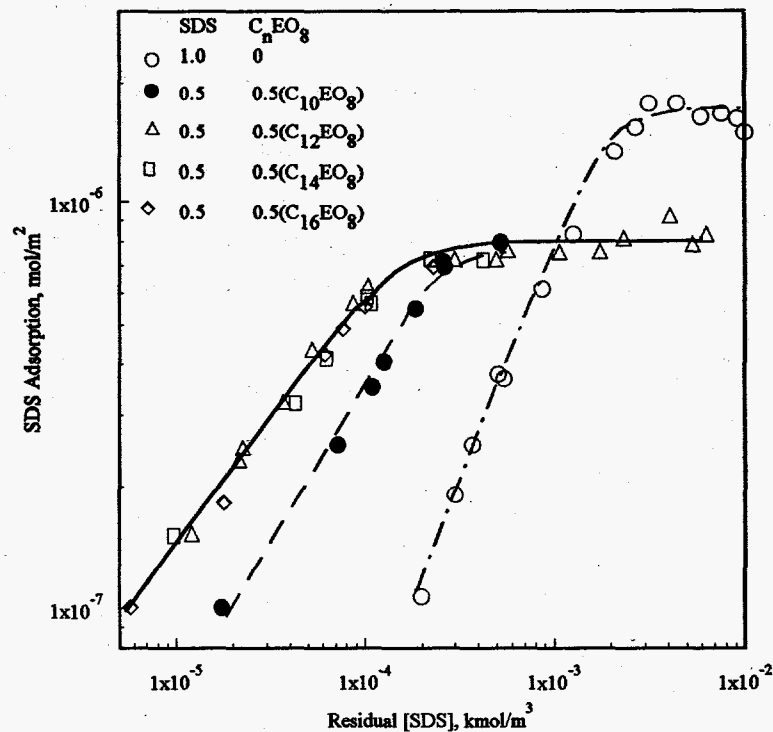


Figure 24 Effect of nonionic surfactant hydrocarbon chain length on the adsorption of sodium dodecyl sulfate (SDS) on kaolinite from 1:1 SDS/ C_nEO_8 mixtures. 0.03 M NaCl, pH 5.

When the hydrocarbon chain length of the nonionic surfactant is shorter ($C_{10}EO_8$) than that of the anionic SDS, however, a different isotherm is obtained. The role of chain length of the nonionic surfactants on kaolinite is illustrated in figure 25.

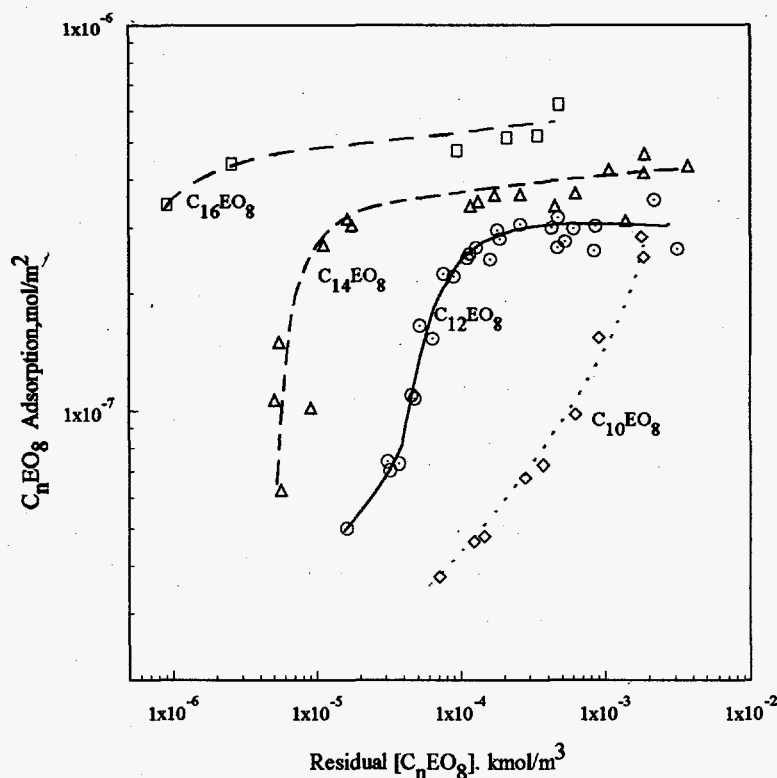


Figure 25 Effect of hydrocarbon chain length (C_nEO_8) on the adsorption of nonionic surfactant on kaolinite. 0.03 M NaCl, pH 5.

It is clear that the chain length has drastic effect on the adsorption. The presence of the anionic SDS enhances the adsorption of the nonionic C_nEO_8 (figure 26) and the isotherms are shifted to lower concentration region as compared to the adsorption isotherms of C_nEO_8 in the absence of any SDS. These results show that the hydrophobic interaction between the coadsorbing surfactants is very strong and a schematic description of the interactions is provided in figure 27.

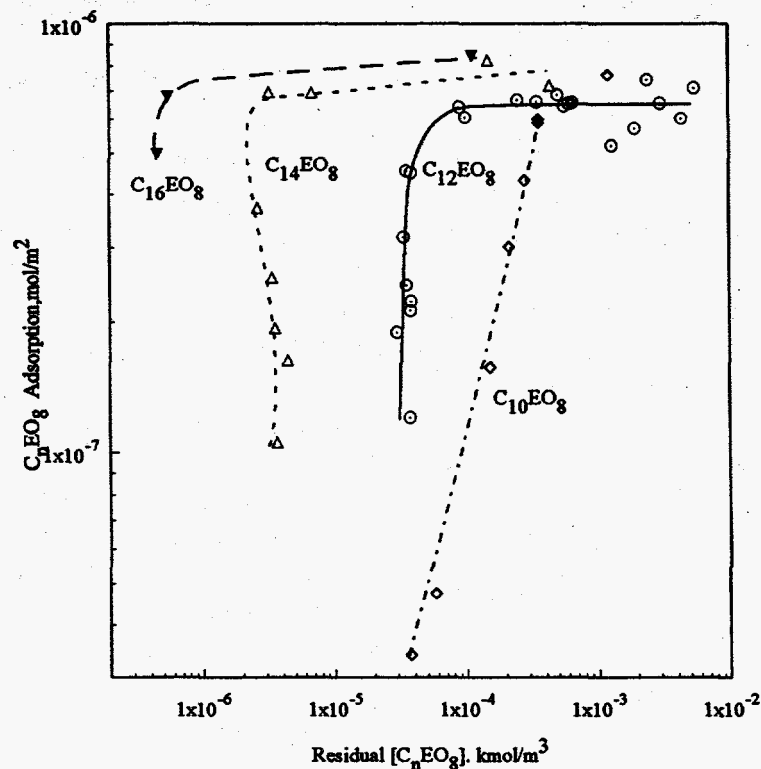


Figure 26 Effect of nonionic surfactant hydrocarbon chain length on the adsorption of C_nEO_8 ($n=10,12,14,16$) on kaolinite from its 1:1 mixtures with SDS. 0.03 M NaCl, pH 5

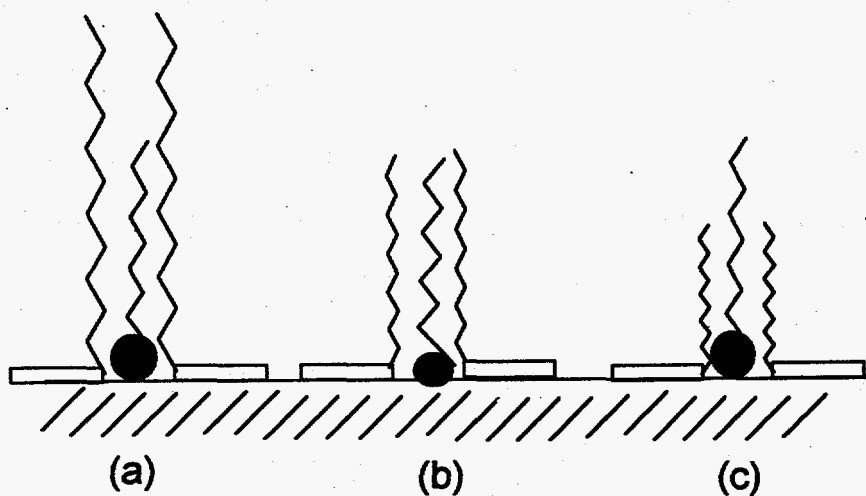


Figure 27 Schematic representation of the effect of nonionic surfactant hydrocarbon chain length on the adsorption of the anionic surfactant SDS when the nonionic surfactant hydrocarbon chain is (a) longer than SDS, (b) equal to SDS and (c) shorter than SDS.

When the hydrocarbon chain length of the nonionic surfactant is equal to or longer than that of the anionic SDS, the hydrocarbon chains of SDS are equally shielded from the hydrophilic

environment by the hydrophobic chains of the coadsorbing nonionic surfactant.

The identical residing environment then leads to a common SDS adsorption isotherm (figure 24). When the hydrocarbon chain of the nonionic surfactant is shorter than that of the anionic sodium dodecyl sulfate (SDS), part of the SDS hydrocarbon chain is exposed to the hydrophilic environment (aqueous solution of the hydrophilic ethylene oxide chain of the nonionic surfactant). The environment for SDS hydrocarbon chain is then less hydrophobic and therefore the isotherm is shifted less to the lower concentration region than in the former case.

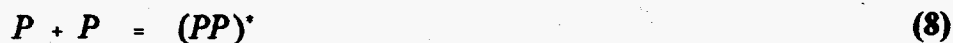
This modification in adsorption characteristics of both surfactants should have a direct impact on the size of the surfactant aggregates bound at the solid-liquid interface and the related interfacial properties. The size of the bound aggregate was determined using fluorescence spectroscopy.

Fluorescence Probing of Mixed-surfactant Adsorbed Layers

Fluorescence spectroscopy could not be conducted at the kaolinite-water interface since kaolinite quenched the fluorescence signal from pyrene. Instead fluorescence probing of the adsorbed layer was performed for adsorption on alumina assuming that the interactions between the surfactants at a different interface would be altered slightly but the trend will be the same. In addition, alumina is a constituent of kaolinite.

In studies conducted during the first year, pyrene monomer fluorescence was used to determine the micropolarity of the adsorbed layer. In addition to the monomer fluorescence, another aspect of pyrene fluorescence, viz. excimer formation, was exploited to determine the size of surfactant aggregates (micelles, hemimicelles, etc). An excimer is formed when a pyrene molecule in its excited state (P^*) interacts with a pyrene molecule in its ground state (P) according to the

reaction:



The excimer formed $(PP)^*$ decays to the ground state by emitting a photon:



In the presence of pyrene molecules in a fragmented media (such as when surfactant micelles, hemi-micelles, etc. are present) the decay of pyrene fluorescence can be fitted to the following model¹⁰ based upon a Poisson distribution of probes in surfactant (or hydrophobic) aggregates:

$$I_t = I_0 \exp \left[-k_o \cdot t + n \left(\exp \{-k_e \cdot t\} - 1 \right) \right] \quad (10)$$

where I_0 is the fluorescence emission intensity at the desired wavelength at time $t=0$, k_o the monomer decay rate constant, k_e the excimer formation rate constant, and n the average number of pyrene molecules in a surfactant aggregate. At long times, there is no excimer formation and the fluorescence decay profiles represent decay due to monomeric emission. Therefore equation 10 reduces to:

$$\ln \left(\frac{I_t}{I_0} \right) = -n - k_o \cdot t \quad (11)$$

and extrapolation to $t=0$ gives n . With a knowledge of n , the aggregation number of the hydrophobic aggregate in which the pyrene molecules reside can be evaluated from the following:

¹⁰ R. Zana, in Surfactant Solutions: New Methods of Investigation, Surfactant Science Series, R. Zana (ed), Vol. 22, Marcel Dekker, New York, 1987.

$$N_{agg} = \frac{n \cdot [C_i - CMC]}{[Py]} \quad \text{for micelles} \quad (12)$$

$$= \frac{n \cdot [C_i - C_r]}{[Py]} \quad \text{for adsorbed layer}$$

where C_i is the initial total surfactant concentration, CMC the critical micelle concentration, $[Py]$ the pyrene concentration and C_r the total residual surfactant concentration.

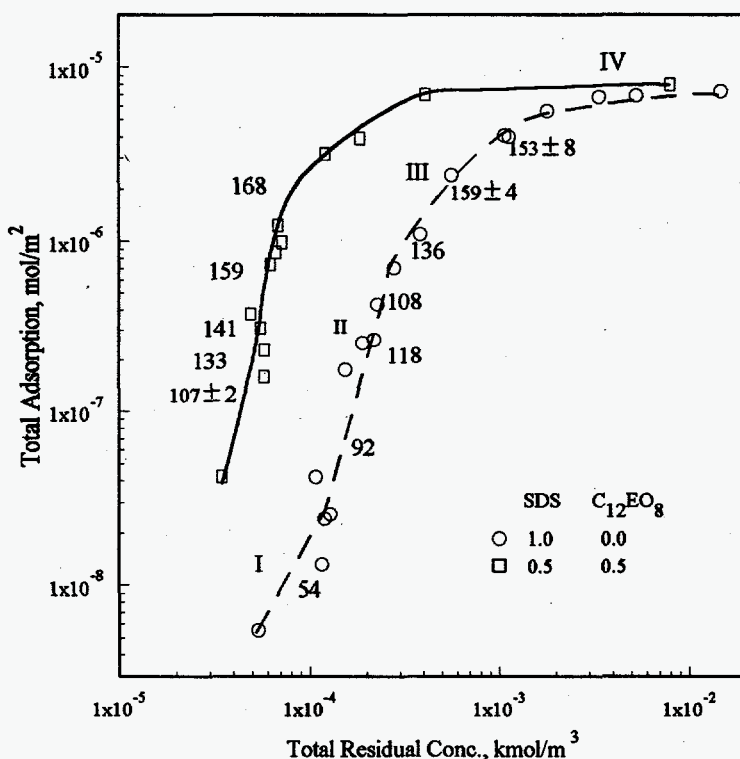


Figure 28 Total adsorption of sodium dodecyl sulfate (SDS) and 1:1 SDS/C₁₂EO₈ mixtures on alumina and aggregation numbers of surfactant.

Using this procedure the aggregation number of a 1:1 SDS/C₁₂EO₈ mixed adsorbed layer was determined and the numbers obtained are given in figure 28 along the adsorption isotherms. It is seen that for SDS adsorption, the aggregation number initially increases and then remains relatively constant in region III. Most importantly, the aggregation number for the adsorption of a 1:1

SDS/C₁₂EO₈ mixture is larger than that for pure SDS adsorption at a similar adsorption density. It is also seen from Table II that the aggregation number for a 1:1 SDS/C₁₂EO₈ micelle is larger than that of SDS micelles.

Table II Aggregation number (N_{agg}) of Surfactant micelles, 0.03 M NaCl, 25°C

SURFACTANT	CONC. (kmol/m ³)	k_o ns ⁻¹	k_e ns ⁻¹	n	N_{agg}
Sodium dodecyl sulfate (SDS)	8.0×10^{-2}	0.0064	0.024	0.88	91
Octaethylene glycol mono n-decyl ether (C ₁₂ EO ₈)	2×10^{-3}	0.0059	0.015	0.53	109±9
1:1 SDS/C ₁₂ EO ₈	8.6×10^{-3}	0.0066	0.012	0.84	165±3

Clearly, the aggregates of the mixed surfactants are larger than the aggregates of the single component and this is proposed to be due to the reduction in electrostatic repulsion between SDS ions due to the presence of the nonionic C₁₂EO₈ for 1:1 SDS/C₁₂EO₈ mixtures in the adsorbed layer or in micelles. As a result of the screening of the electrostatic repulsion, the adsorption of sodium dodecyl sulfate (SDS) should be energetically enhanced. This is indeed seen from figure 29.

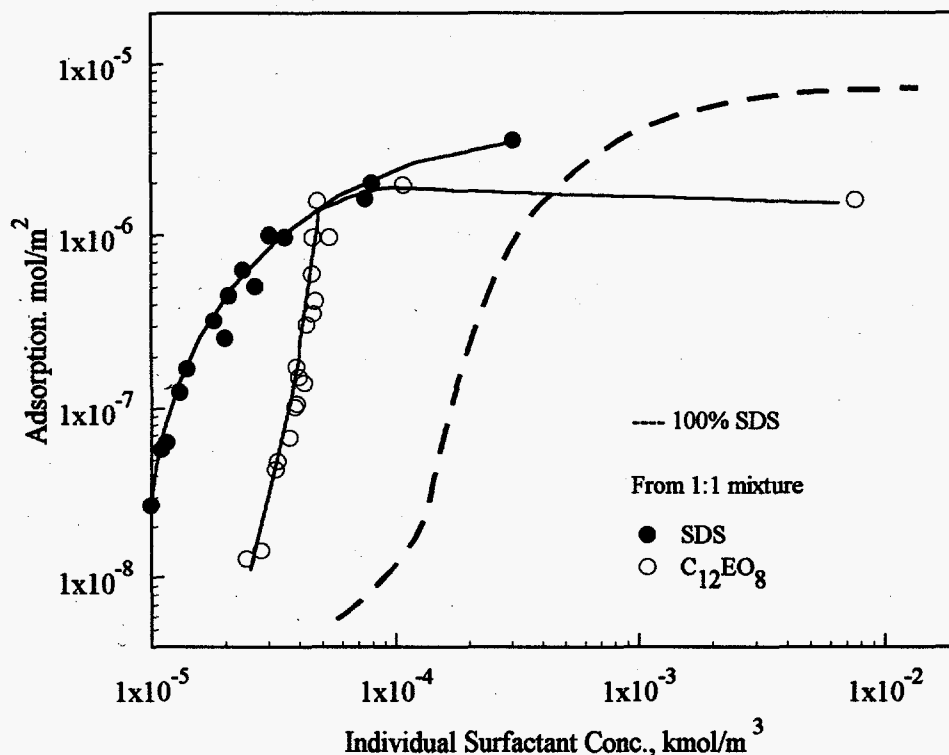


Figure 29 Isotherms for individual surfactant adsorption on alumina from 1:1 SDS/C₁₂EO₈ mixtures.

Since the mixed aggregates consist of both the anionic sodium dodecyl sulfate (SDS) and the nonionic octaethylene glycol mono n-decyl ether (C₁₂EO₈), it is useful to determine the aggregation number for each surfactant in the mixed aggregates. This can be done by knowing the adsorption density of each component in the mixed adsorbed layer. It is seen from Table III that at low adsorption densities, the aggregation number of the nonionic octaethylene glycol mono n-decyl ether (C₁₂EO₈) species is lower than that of the anionic SDS. As the adsorption increases, however, the hydrophobic chain-chain interaction becomes more important and the aggregation number of each surfactant becomes similar to each other.

Table III Surfactant aggregation number (N_{agg}) for the adsorption of 1:1 SDS/ $C_{12}EO_8$ mixture on alumina: 0.03 M NaCl, pH 6.5, 25°C

ADS. (kmol/m ³)	SURF./PY	k_o	k_e ns ⁻¹	n ns ⁻¹	SDS	N_{agg} $C_{12}EO_8$	TOTAL
1.1×10^{-7}	157	0.015	0.18	0.68	61	46	107
2.3×10^{-7}	173	0.013	0.055	0.77	72	61	133
3.2×10^{-7}	179	0.01	0.015	0.79	74	67	141
6.2×10^{-7}	187	0.0079	0.011	1.60	82	77	158
1.9×10^{-6}	194	0.0071	0.0055	0.86	85	83	168

It is to be noted that the aggregation number for SDS in the mixed adsorbed layer is lower than that for pure sodium dodecyl sulfate (SDS) adsorption. This can be explained by considering the surface heterogeneity. Since the surface consists of energetic patches¹¹ for SDS adsorption and since the nonionic $C_{12}EO_8$ does not adsorb on alumina by itself, the aggregate size should be largely limited by the finite size of the energetic patches for SDS adsorption. In the case of 1:1 SDS/ $C_{12}EO_8$ adsorption, part of the SDS ions will be displaced by the nonionic $C_{12}EO_8$ in order to co-adsorb and as a result the aggregation number of SDS is decreased.

¹¹ J.H. Harwell, J.C. Hoskins, R.S. Schechter and W.H. Wade, *Langmuir*, 1, 1985, 251.

SUMMARY

Adsorption/desorption of single surfactants and surfactant mixtures was studied on solids relevant to reservoir minerals. Adsorption/desorption of tetradecyltrimethylammonium chloride (TTAC) was studied at the alumina-water interface and significant hysteresis was observed at low surfactant concentration. Also upon dilution the nature of the adsorbed layer was altered, and during desorption aggregates were present even at residual concentrations where no such aggregates formed during adsorption. It appears that the initial aggregates rearrange and do not desorb. This led to some hysteresis at lower concentrations.

Interactions between dissimilar surfactants (cationic and nonionic) modified the adsorption behavior of both the cationic (tetradecyl trimethyl ammonium chloride - TTAC) and the nonionic (pentadecylethoxylated nonyl phenol NP-15) surfactants. In the presence of TTAC, adsorption of NP-15 was induced on the substrate (alumina) where it normally does not adsorb. The presence of NP-15 lowered the adsorption of TTAC due to the shielding of the electrostatic interactions between the cationic surfactant and anionic substrate (pH 10). Desorption of TTAC in mixtures with low amounts of NP-15 was similar to that of TTAC alone. Since NP-15 adsorption required the anchoring presence of TTAC, the desorption was also dependent upon TTAC desorption. In NP-15 rich mixtures, the desorption behavior was more complex and mechanisms have yet to be elucidated. Regular solution theory was used to model the interactions between NP-15 and TTAC in solution. From the value of the interaction parameter it was evident that the interactions were not strong. Monomer concentration of mixtures were calculated and attempts made to correlate them with their adsorption behavior. Adsorption of TTAC was found to be dependent upon monomer concentrations but there was no such relation for NP-15 since its adsorption was dependent upon preadsorbed

TTAC.

In addition to the cationic-nonionic system, interactions between an anionic surfactant (sodium dodecyl sulfate - SDS) and a nonionic surfactant (octaethylene glycol mono-n-dodecyl ether - $C_{12}EO_8$) with varying hydrocarbon chain length were also studied. Hydrophobic chain-chain interactions led to enhanced adsorption of both surfactants. Interestingly, once the hydrocarbon chain length of the nonionic surfactant exceeded that of the anionic surfactant there was no further enhancement of SDS adsorption.

Aggregate size of 1:1 mixtures of SDS/ $C_{12}EO_8$ adsorbed at the alumina-water interface was measured using dynamic pyrene fluorescence spectroscopy. Presence of the nonionic surfactant in the mixed aggregate with the anionic SDS reduced the electrostatic repulsion and increased the total aggregate size. The SDS aggregate at the interface was smaller than that of the $C_{12}EO_8$ aggregate for similar adsorption densities. Also the number of SDS molecules in the mixed aggregate was smaller than that of the single component aggregate. The differences in the aggregate structure during adsorption and desorption can also be expected to cause differences in the interfacial properties such as wettability and dispersion of the mineral particles.

In conclusion, interactions between ionic and nonionic surfactants have been exploited to modify the solution and interfacial properties of the individual surfactants. Aggregate size, reduction of interfacial tension and adsorption/desorption characteristics were all modified by a judicious selection of surfactant combinations. These findings have important bearings because commercial surfactants invariably are mixtures.